ISSN 2096-7071 (Print)
ISSN 2096-3101 (Online)
CN 10-1629/R1

CHINA CDC WEEKLY

Vol. 6 No. 12 Mar. 22, 2024

中国疾病预防控制中心周报

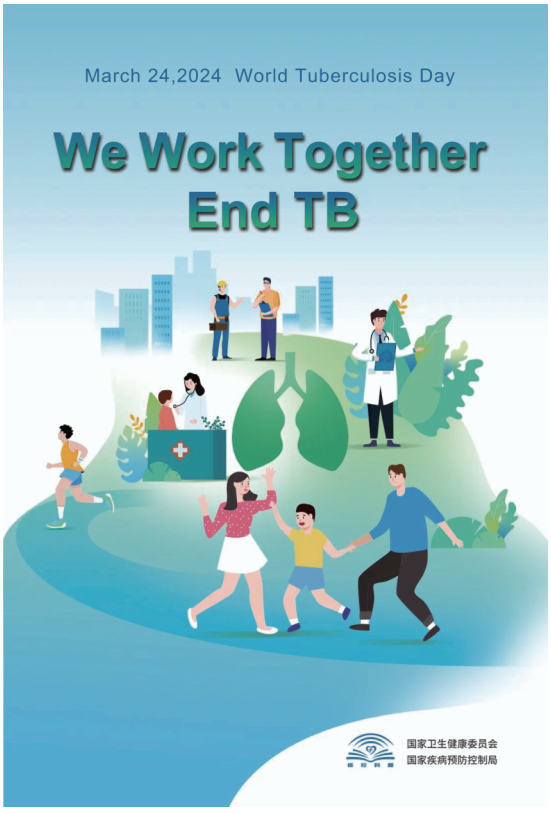

ISSN 2096-7071
9 772096 707248 12>

China CDC Weekly

Cover Image: adapted from National Disease Control and Prevention Administration, https://www.ndcpa.gov.cn/jbkzzx/c100008/common/content/content_1765985611639595008.html.

Preplanned Studies

Tuberculosis Prevalence Trends from a Predictive Modelling Study — 10 High-Burden Countries, 1980–2035

Qiuping Chen[1,2,&]; Qiao Liu[3,&]; Kangguo Li[4,&]; Laurent Gavotte[5]; Roger Frutos[1,#]; Tianmu Chen[3,4,#]

Summary

What is already known about this topic?

Given the challenges presented by drug-resistant strains of tuberculosis (TB) and the rising mobility of the population, achieving the objective of eradicating TB appears uncertain.

What is added by this report?

The examination of TB incidence trends in 10 high-burden countries (HBCs) indicated a steady rise in cases, with India and China jointly accounting for nearly 70% of the burden. Projections for the future show diverse trajectories in these countries, with potential difficulties in reaching the TB elimination target, especially in Nigeria, Congo, and South Africa.

What are the implications for public health practice?

The number of TB cases is on the rise. It is crucial to learn from successful strategies to improve TB prevention and control worldwide through collaborative efforts.

The fight against tuberculosis (TB) is being severely hampered by the development of drug-resistant strains and increased human mobility, further compounded by the impact of the coronavirus disease 2019 (COVID-19) pandemic (*1*). The World Health Organization (WHO) Post-2015 End TB Strategy, which was endorsed by the World Health Assembly in 2014 and aligns with the Sustainable Development Goals, has the ambitious objective of eradicating the global TB epidemic (*2*). Nonetheless, there is growing concern regarding the adequacy of existing TB control strategies to meet these objectives. This study employed four predictive models to evaluate the likelihood of reaching the WHO's targets within a set timeframe, specifically examining the situation in the 10 high-burden countries (HBCs). Our findings indicate a worsening global TB burden, with numerous countries falling short of the aspirations to eliminate pulmonary TB. Therefore, it is imperative to draw on successful strategies and enact tailored interventions within key nations in conjunction with bolstered international collaboration.

TB case data were extracted from the WHO Global Tuberculosis Programme's open data repository (https://www.who.int/teams/global-tuberculosis-programme/data), while demographic details, including population size, were gathered from the World Bank's open data platform. An incidence analysis of TB was carried out for 10 HBCs spanning from 1980 to 2021. It is predicted that China, Congo, India, Indonesia, Mozambique, Myanmar, Nigeria, the Philippines, South Africa, and Zambia will continue to rank among the top 30 HBCs until 2023 due to the persistent challenges of drug-resistant TB and TB/human immunodeficiency virus (HIV) co-infection (*1*,*3*).

In order to predict TB incidence for the years 2023–2035, various predictive models were utilized, including the autoregressive integrated moving average (ARIMA) model (*4*), neural network model (*5*), bayesian structural model (*6*), and a hybrid model integrating ARIMA, exponential smoothing (ETS), and seasonal and trend decomposition using Loess (STL). Details on these models can be found in the Supplementary Material (available at https://weekly.chinacdc.cn/). Data analysis was conducted using R software (version 4.3.3, R Core Team, Vienna, Austria).

Figure 1 depicts the trend of TB incidence in the 10 HBCs from 1980 to 2022. These 10 nations collectively account for 117,314,803 TB cases, representing 60% of the global total. The number of TB cases in the 10 HBCs has been increasing annually, with the exception of a decline in 2020 and 2021 due to the COVID-19 pandemic. Among these countries, nearly 70% of TB cases are concentrated in India and China, highlighting the urgent need to address the TB burden in these two nations. India has consistently shown the highest TB incidence over the past 43 years, with a rising trend since the publication of the TB report in 1997. In contrast, while China has a considerable TB incidence rate, it has been steadily

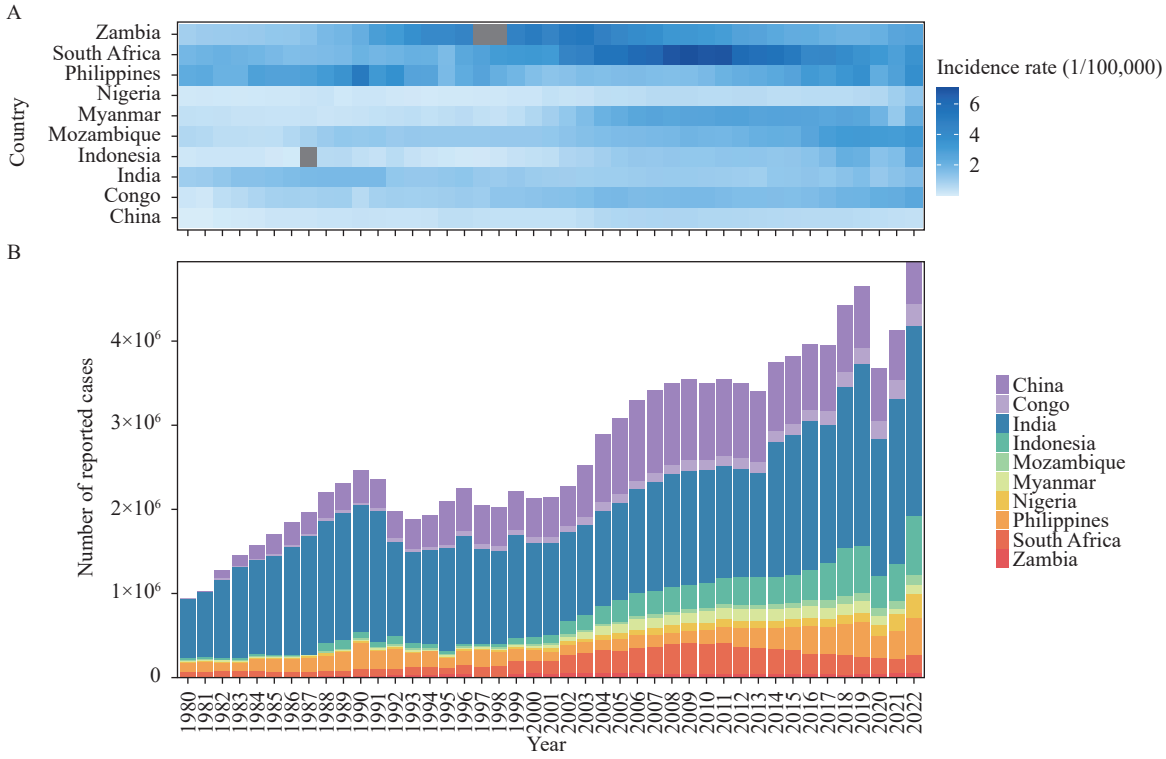

FIGURE 1. The spatiotemporal distribution characteristics of global tuberculosis.

decreasing since 2009, as evidenced in the graph depicting incidence patterns (Figure 1B).

To conduct a thorough analysis of TB incidence trends, we utilized four different models to predict TB cases from 2023 to 2035 (Figure 2). The results revealed a decreasing trend in future TB cases in China, as projected by three of the four models, with the exception of the neural network model. Conversely, Congo is expected to see a rise in TB cases over the next 13 years, regardless of the forecasting model employed. Similar patterns were observed for India, the Philippines, and Zambia, where the bayesian model anticipated a significant increase, while the other models predicted relatively stable case numbers. In the case of Mozambique and Nigeria, the ARIMA, bayesian, and hybrid models foresee a surge in TB cases, while the neural network model predicts minimal changes. South Africa's future TB incidence shows divergent forecasts, with the ARIMA model suggesting stability and the remaining models indicating an increase. Myanmar's projections also vary, with the bayesian model forecasting a decline while the other models predict minimal changes. Indonesia poses significant differences among the models, with the ARIMA and bayesian models forecasting a notable increase, while the hybrid and Neural Network models suggest periodic fluctuations in TB cases. When considering forecasts based on pre-COVID-19 data using the four models (Supplementary Figure S1, available at https://weekly.chinacdc.cn/), it was noted that apart from Congo, Mozambique, and Nigeria, the forecast outcomes for other countries were influenced to varying degrees by the COVID-19 pandemic. For instance, the impact of COVID-19 has altered the upward trend in India and lessened the decline in China, and all models for Indonesia now predict an increase in TB cases.

Figure 3 and Supplementary Figure S2 (available at https://weekly.chinacdc.cn/) present a detailed overview of the projected TB case trends in the 10 HBCs aimed at reaching the goal of TB elimination. Besides China, which is forecasted to meet the TB elimination target according to the bayesian model, the other countries are unlikely to reach the desired goal across all forecasting models due to the impact of COVID-19. Excluding the influence of COVID-19, only the forecast results for South Africa based on the bayesian model indicate potential success in achieving this goal.

DISCUSSION

This study suggests that a majority of countries are

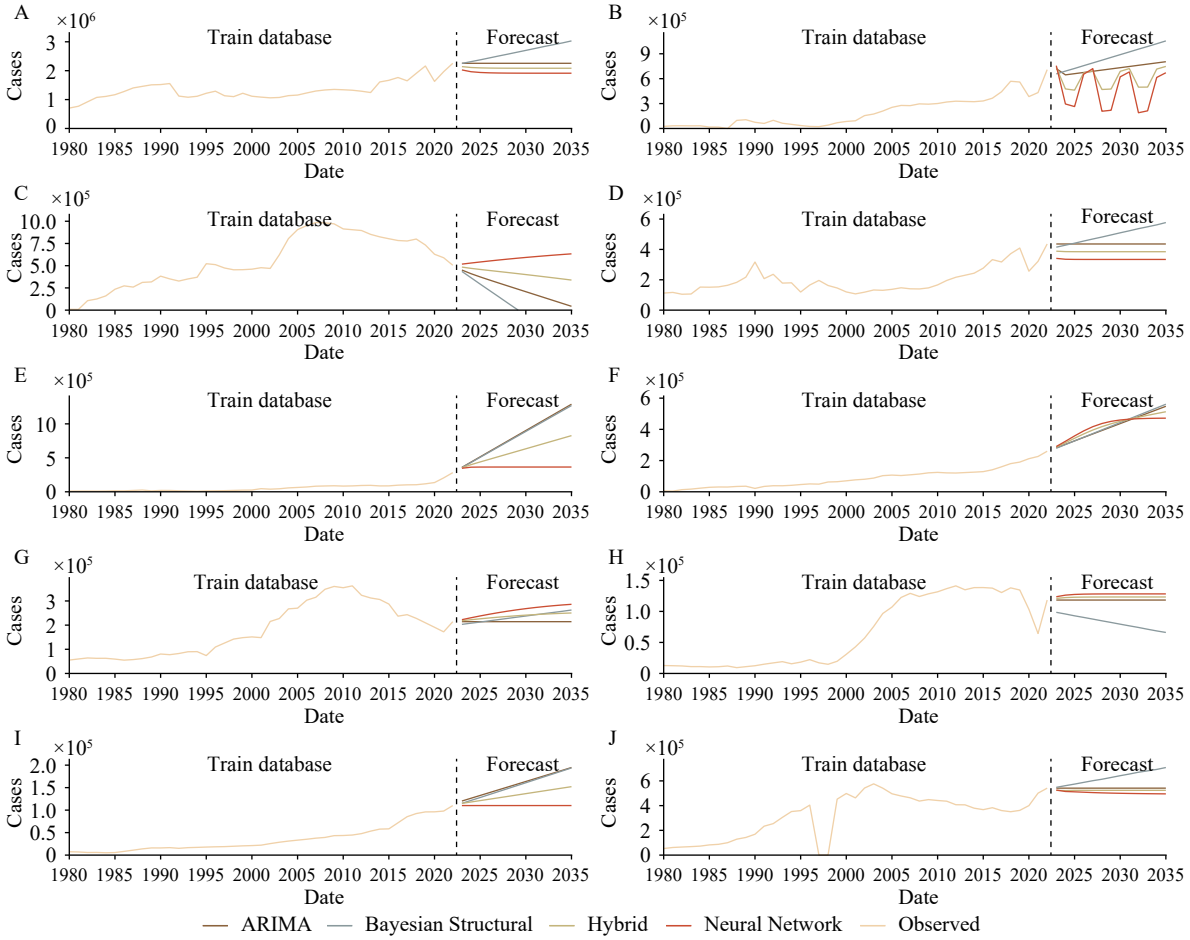

FIGURE 2. Time trends forecasted by four models in ten HBCs. (A) India; (B) Indonesia; (C) China; (D) Philippines; (E) Nigeria; (F) Congo; (G) South Africa; (H) Myanmar; (I) Mozambique; (J) Zambia.
Abbreviation: HBC=high-burden countries.

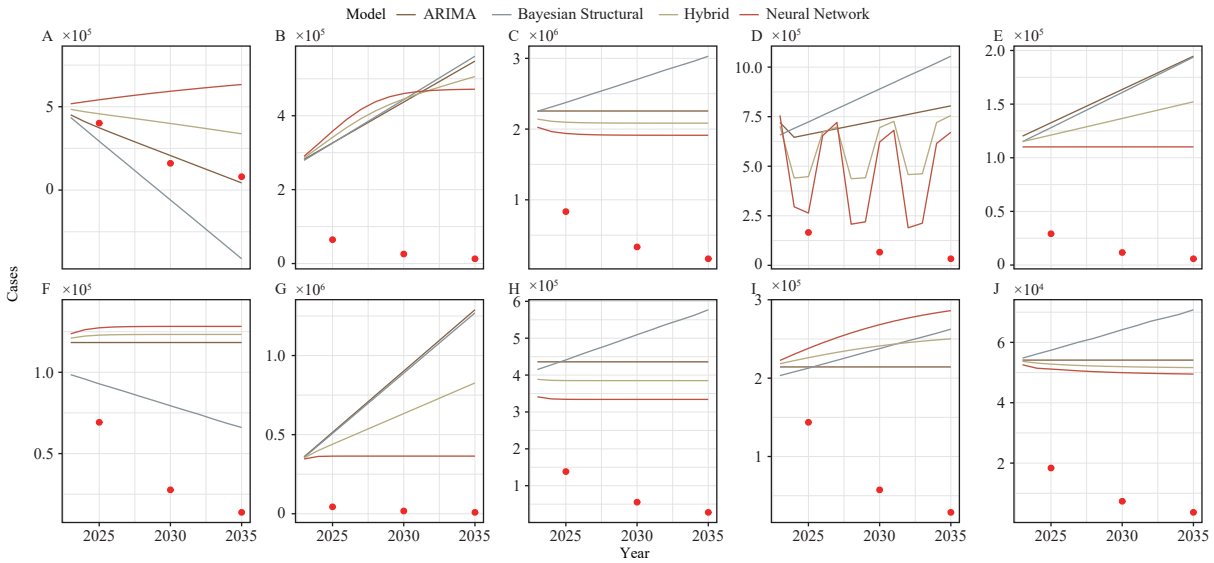

FIGURE 3. Accessibility projections for ten HBCs to achieve the goal of ending tuberculosis based on four models. (A) China; (B) Congo; (C) India; (D) Indonesia; (E) Mozambique; (F) Myanmar; (G) Nigeria; (H) Philippines; (I) South Africa; (J) Zambia.

projected to experience a sustained rise in TB cases from 2023 to 2035. The endeavor to eliminate pulmonary TB poses a significant challenge, underscoring the imperative for enhanced implementation of pertinent interventions.

Within the 10 HBCs, the projections for TB are discouraging. These countries, which are on all three of the major burden lists, contribute to over 60% of the global TB cases reported. India, in particular, has the highest TB incidence rate and is experiencing an annual increase. This underlines the urgent need for India to enhance its TB management strategies. The 2023 Global TB Report also highlights that China continues to be a country heavily afflicted by TB, with an estimated 748,000 cases in 2022, trailing only behind India, with 2.82 million cases, and Indonesia, with 1.06 million cases. Although models project a reduction in TB occurrences in China, a considerable divergence persists from the target to eliminate TB. Furthermore, projections indicate an increase in TB cases for the remaining eight countries, posing a serious challenge for TB prevention and control. Model predictions reflect varying degrees of influence by the COVID-19 pandemic, which may be attributed to alterations in population behaviors, implementation of preventive strategies, and data collection and quality issues during the pandemic. These factors introduce potential uncertainties and biases into the predictive models. Consequently, it is critical to meticulously consider the impact of the COVID-19 pandemic when estimating future TB rates to ensure that the projections are accurate and dependable (*1*,*3*).

The burden of TB in the 10 HBCs is significant, further complicated by issues like drug-resistant strains and the co-infection of TB with HIV. These nations are vital in the global fight against TB, with their struggles and achievements holding crucial insights for worldwide TB control endeavors. Between 2016 and 2020, Russia made notable strides in TB prevention and control, meeting the WHO's targets for 2020. This progress was linked to the implementation of new diagnostic tools, successful treatment protocols, expanded population coverage for TB screening, and the establishment of healthcare programs supporting TB patients, particularly those with HIV co-infection (*7*). With the challenges faced by these HBCs in achieving the goals of the End Tuberculosis Strategy, there is an immediate need to learn from their accomplishments and fortify global TB prevention and control measures. This entails embracing technological innovations, enforcing effective regulations, refining strategic frameworks, and enhancing service-oriented schemes.

This study is subject to some limitations. The analysis utilizes notification data from the WHO online database, which could fluctuate due to changes in national surveillance systems, potentially impacting underreporting and missed diagnoses. Consequently, these data may not entirely reflect the actual trends in TB incidence, particularly over prolonged periods. Additionally, our predictive modeling is assumption-based and susceptible to influences such as policy changes and healthcare infrastructure.

In conclusion, the burden of TB is increasing in the 10 HBCs, particularly in India, Indonesia, and China. Variations exist among prediction models, with the predictions being impacted to varying degrees by the COVID-19 pandemic. Attaining the target of eradicating TB is proving to be difficult for many countries. These results highlight the necessity of tailored interventions and continuous initiatives to manage TB, especially in countries with substantial upward trends like Indonesia, Nigeria, and Congo. Additionally, they stress the importance of enhanced international collaboration.

Conflicts of interest: The funder had no role in the study design, data collection and analysis, decision to publish, or manuscript preparation. No other conflicts of interest.

Funding: This study was supported by Self-supporting Program of Guangzhou Laboratory (grant number: No. SRPG22-007).

doi: 10.46234/ccdcw2024.045

[#] Corresponding authors: Tianmu Chen, chentianmu@xmu.edu.cn; Roger Frutos, frutossmt@gmail.com.

[1] CIRAD, Intertryp, Montpellier, France; [2] Université de Montpellier, Montpellier, France; [3] State Key Laboratory of Molecular Vaccinology and Molecular Diagnostics, National Innovation Platform for Industry-Education Integration in Vaccine Research, Xiamen University, Xiamen City, Fujian Province, China; [4] State Key Laboratory of Vaccines for Infectious Diseases, Xiang An Biomedicine Laboratory, School of Public Health, Xiamen University, Xiamen City, Fujian Province, China; [5] Espace-Dev, Université de Montpellier, Montpellier, France.

[&] Joint first authors.

Submitted: March 06, 2024; Accepted: March 15, 2024

REFERENCES

1. World Health Organization. Global tuberculosis report 2022. 2022. https://www.who.int/teams/global-tuberculosis-programme/tb-reports/global-tuberculosis-report-2022. [2023-12-21].
2. World Health Organization. The end TB strategy. 2015. https://www.who.int/teams/global-tuberculosis-programme/the-end-tb-strategy.

[2023-12-21].
3. World Health Organization. Global tuberculosis report 2023. 2023. https://www.who.int/publications/i/item/9789240083851.[2023-12-21].
4. Yan CQ, Wang RB, Liu HC, Jiang Y, Li MC, Yin SP, et al. Application of ARIMA model in predicting the incidence of tuberculosis in China from 2018 to 2019. Chin J Epidemiol 2019;40(6):633 – 7. https://doi.org/10.3760/cma.j.issn.0254-6450.2019.06.006.
5. Li ZM, Li YN. A comparative study on the prediction of the BP artificial neural network model and the ARIMA model in the incidence of AIDS. BMC Med Inform Decis Mak 2020;20(1):143. https://doi.org/10.1186/s12911-020-01157-3.
6. Paramasivan K, Sudarsanam N. Impact of COVID-19 pandemic on road safety in Tamil Nadu, India. Int J Inj Contr Saf Promot 2022;29(2):265 – 77. https://doi.org/10.1080/17457300.2021.2007134.
7. Starshinova A, Dovgalyk I, Beltukov M, Zinchenko Y, Glushkova A, Starshinova AY, et al. Tuberculosis in the Russian federation: dynamics of the epidemic indicators before and after COVID-19 pandemic. Life 2022;12(10):1468. https://doi.org/10.3390/life12101468.

SUPPLEMENTARY MATERIAL

Methods

The Autoregressive Integrated Moving Average (ARIMA) model was specified as ARIMA (p, d, q), where p represents autoregressive terms, d is the number of differences for stationarity, and q shows the moving average terms. Model selection was based on the Akaike Information Criterion. The bayesian structural model was implemented using Markov chain Monte Carlo sampling to estimate the posterior distribution of the time series parameters. The neural network model comprised an ensemble of 20 networks, each with randomly initialized weights, trained for one-step forecasting and recursively applied for multi-step predictions.

When attempting to forecast future trends in tuberculosis case reports using time series models, the selection of appropriate models is crucial. The rationale behind choosing the "bayesian structural," "ARIMA," and the hybrid model combining elements of "neural network" with seasonal autoregressive integrated moving average (SARIMA), exponential smoothing (ETS), and seasonal and trend decomposition using Loess (STL) components is based on their unique strengths and capabilities in capturing different aspects of time series data.

The bayesian structural model was chosen for its ability to incorporate prior knowledge and uncertainty into the modeling process. By leveraging bayesian inference, this model can provide more robust estimates and predictions, especially when dealing with complex data patterns and structural changes over time.

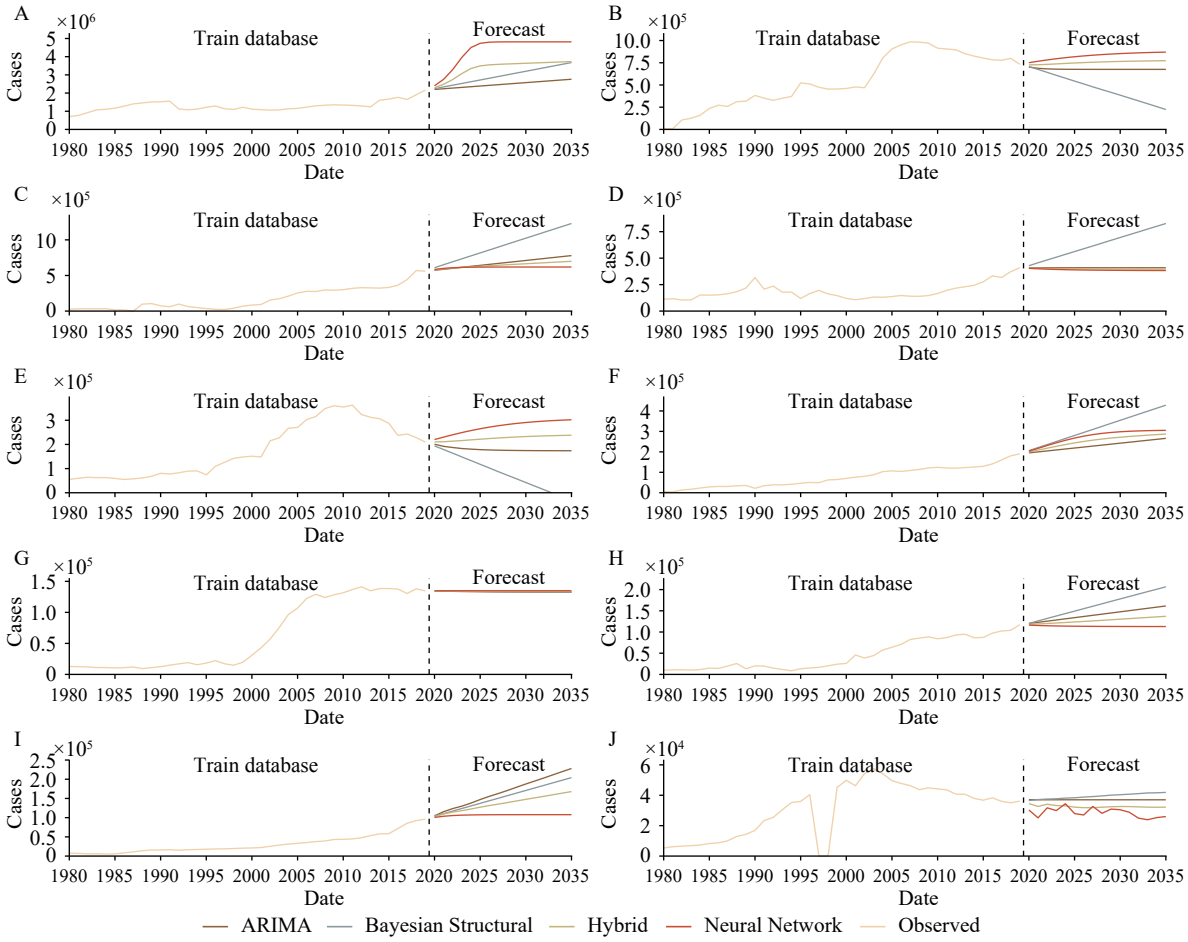

SUPPLEMENTARY FIGURE S1. Results of Four Model Fits and Predictions 10 HBCs during the pre-COVID-19 Era. (A) India; (B) China; (C) Indonesia; (D) Philippines; (E) South Africa; (F) Congo; (G) Myanmar; (H) Nigeria; (I) Mozambique; (J) Zambia.

Abbreviation: HBC=high-burden countries; ARIMA=autoregressive integrated moving average; COVID-19=coronavirus disease 2019.

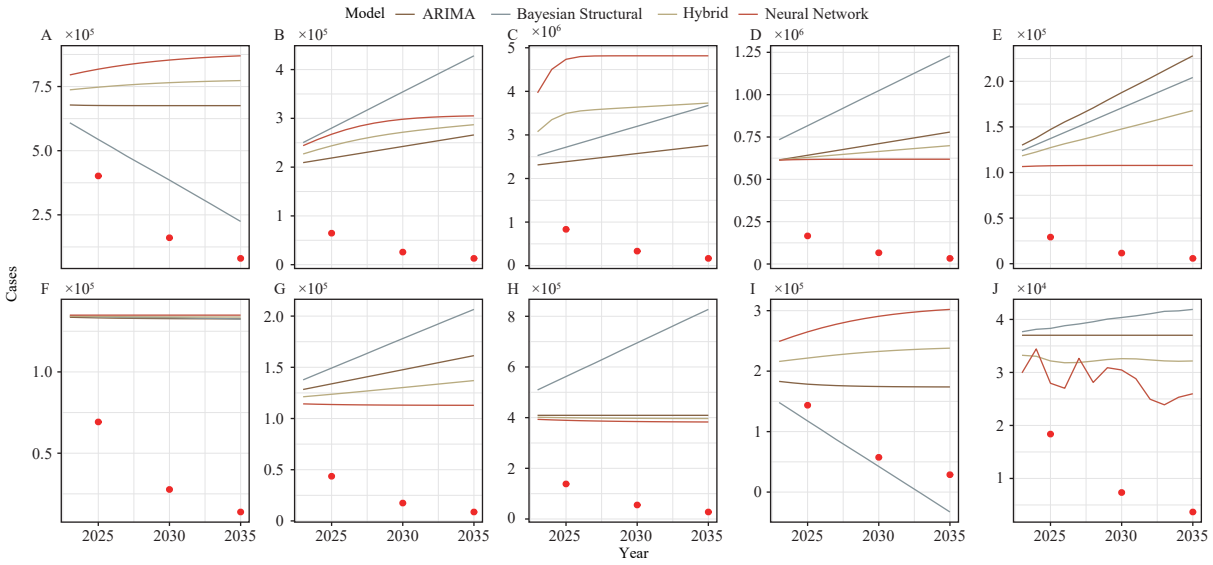

SUPPLEMENTARY FIGURE S2. Feasibility of Ending Tuberculosis during pre-COVID-19 predictions for 10 high-burden countries. (A) China; (B) Congo; (C) India; (D) Indonesia; (E) Mozambique; (F) Myanmar; (G) Nigeria; (H) Philippines; (I) South Africa; (J) Zambia.
Abbreviation: HBC=high-burden countries; ARIMA=autoregressive integrated moving average; COVID-19=coronavirus disease 2019.

ARIMA model is a classic choice for time series forecasting due to its effectiveness in capturing linear dependencies and stationary patterns in the data. It is particularly useful when the data exhibit trends and seasonal variations that can be modeled through autoregressive and moving average components.

The neural network model was chosen for its ability to capture nonlinear relationships and complex dependencies in the data, offering flexibility to model patterns that may not be captured effectively by traditional time series models like ARIMA.

The hybrid model integrates SARIMA, ETS, and STL components with neural network components to leverage the strengths of each approach. SARIMA and ETS can handle seasonality and trend components well, while STL can capture irregular patterns. The neural network component enhances the model's capability to capture nonlinear relationships and complex dependencies in the data.

In summary, the selection of the bayesian structural model, ARIMA model, neural network model, and the hybrid model that combines SARIMA, ETS, and STL with neural network components is based on the diverse strengths of these models in capturing different aspects of the tuberculosis case reports data, including linear dependencies, nonlinear relationships, seasonal patterns, trends, irregularities, and structural changes. This comprehensive approach aims to improve the accuracy and robustness of the forecasting process for tuberculosis case reports.

Preplanned Studies

Molecular Epidemiological Study of a Human Brucellosis Outbreak — Weihai City, Shandong Province, China, 2022

Yan Li[1,&]; Yifan Yu[2,&]; Jian Zhao[3,&]; Shujun Ding[1]; Guoying Zhang[3]; Xiaolin Yu[1]; Zengqiang Kou[1,#]

Summary

What is already known about this topic?

Brucellosis, mainly caused by *Brucella melitensis* (*B. melitensis*), is regarded as a significant zoonotic disease in China. In Weihai, located at the eastern end of the Shandong Peninsula, brucellosis has been in a low epidemic phase for the past five years.

What is added by this report?

This was the initial report of a brucellosis outbreak in the last five years. Strains of *B. melitensis* bv. 3 from Weihai and other cities showed a close genetic relationship, suggesting a potential common ancestry.

What are the implications for public health practice?

Epidemiological investigations depend on standardized and effective molecular typing methods and analysis tools for public health laboratories to identify and trace outbreaks. Understanding the circulation patterns of livestock in free-range households in heavily affected areas is essential for controlling the spread of brucellosis.

The incidence of human brucellosis is closely linked to interaction with infected animals, either through direct contact with those animals or by consuming products from infected livestock. The tracing of epidemiological sources is complicated due to the frequent movement of livestock between provinces and the variety of trade channels. From 2017 to 2022, Weihai experienced a low incidence of brucellosis, averaging 0.6365 cases per 100,000 inhabitants. During the period of June 12 to June 30, 2022, the Weihai CDC identified an outbreak comprising six brucellosis cases. The epidemiological investigation was unable to determine the precise source and route of infection. Advanced techniques such as Multiple Locus Variable-Number Tandem Repeat Analysis (MLVA) and whole genome single nucleotide polymorphism (wgSNP) analyses, utilizing data from whole genome sequencing (WGS), can offer a more definitive resolution in identifying the source of infection, potentially reducing the need for costly field investigations. Survey findings indicated that the outbreak was primarily due to live animal transport from adjacent cities and counties. Implementing novel technologies such as WGS and fostering inter-regional collaboration are essential strategies for curtailing the further transmission of brucellosis.

Whole blood samples were collected from all patients associated with the 2022 outbreak in Weihai, as well as from sporadic cases for strain isolation. The isolates underwent biochemical identification and BCSP31-polymerase chain reaction (BCSP31-PCR). Slide agglutination with monospecific anti-*Brucella* sera and AMOS-PCR were used for biotyping (*1*). Genomic DNA was extracted from the *Brucella* strains using the TIANamp Bacteria DNA Kit (TIANGEN, Beijing, China). The lineages and molecular typing of these strains were determined through MLVA as detailed in previous studies (*2*). The resulting strains were analyzed, and dendrograms were constructed with BioNumerics (version 8.0, Applied Maths, Sint-Martens-Latem, Belgium), utilizing the categorical coefficient and unweighted pair group method using the arithmetic mean (UPGMA) algorithm. WGS was performed for all strains by Novogene Bioinformatics Technology Co., Ltd, employing an Illumina NovaSeq 6000 system (PE, 150 bp reads). *Brucella melitensis* (*B. melitensis*) genomes were aligned against the reference sequence of *B. melitensis* bv. 1 strain 16M (RefSeq GCF_000007125.1) using CLC Genomics Workbench (version 23.0.3, Qiagen, Hilden, Germany) for SNP analysis. Data from MLVA-11, which were completely identical for strains in Shandong Province in 2022, served as the reference for Most Small Tree (MST) and SNP tree construction.

From June 12 to 30, 2022, the China Infectious Disease Surveillance and Reporting Information System detected 4 confirmed cases (patients 1–4) of brucellosis in the Huancui District of Weihai. Through active searches, 2 suspected cases (patients 5–6) were identified and later confirmed by laboratory tests. The outbreak involved a total of 6 cases: 4 cases

(patients 3–6) were involved in livestock husbandry on the same farm, while 2 cases (patients 1–2) contracted the disease by consuming sheep placentas purchased from the farm. An epidemiological investigation revealed that a breeding ram bought from Rushan in August 2021 was likely the source of the infection.

In 2022, six strains were isolated in Weihai. Three strains, identified as 2022SD184, 2022SD185, and 2022SD186, were associated with patients 1, 3, and 6, respectively. The remaining strains, 2022SD060, 2022SD183, and 2022SD510, represented sporadic cases from Wendeng, Rushan, and Rongcheng, respectively. The identification of these strains as *B. melitensis* bv. 3 was confirmed via slide agglutination with monospecific anti-*Brucella* sera and AMOS-PCR. MLVA-11 analysis, which targets 11 specific *Brucella* loci, classified them as belonging to the East Mediterranean lineage and type 116. We expanded our molecular typing approach with additional loci for MLVA, and MST analysis using MLVA-16 data revealed the genetic distance between Weihai's outbreak and sporadic strains (Figure 1). Two distinct MLVA-16 profiles were determined for the outbreak strains. 2022SD185 differed at one locus (bruce 09) compared to the other two strains. Furthermore, identical MLVA-16 profiles were observed among strains 2022SD184, 2022SD186, 2022SD357, and 2022SD620 from Weihai, Zibo, and Yantai cities when compared with 2022 monitoring data of Shandong Province.

WGS of 44 *Brucella melitensis* isolates from Shandong Province revealed 5,159 SNPs. A threshold of seven SNP differences was utilized to identify potentially related strain complexes (*3*). The analysis demonstrated that the three strains implicated in this outbreak differed by a single SNP, corroborating the epidemiological investigation outcomes and confirming their identification as an outbreak cluster.

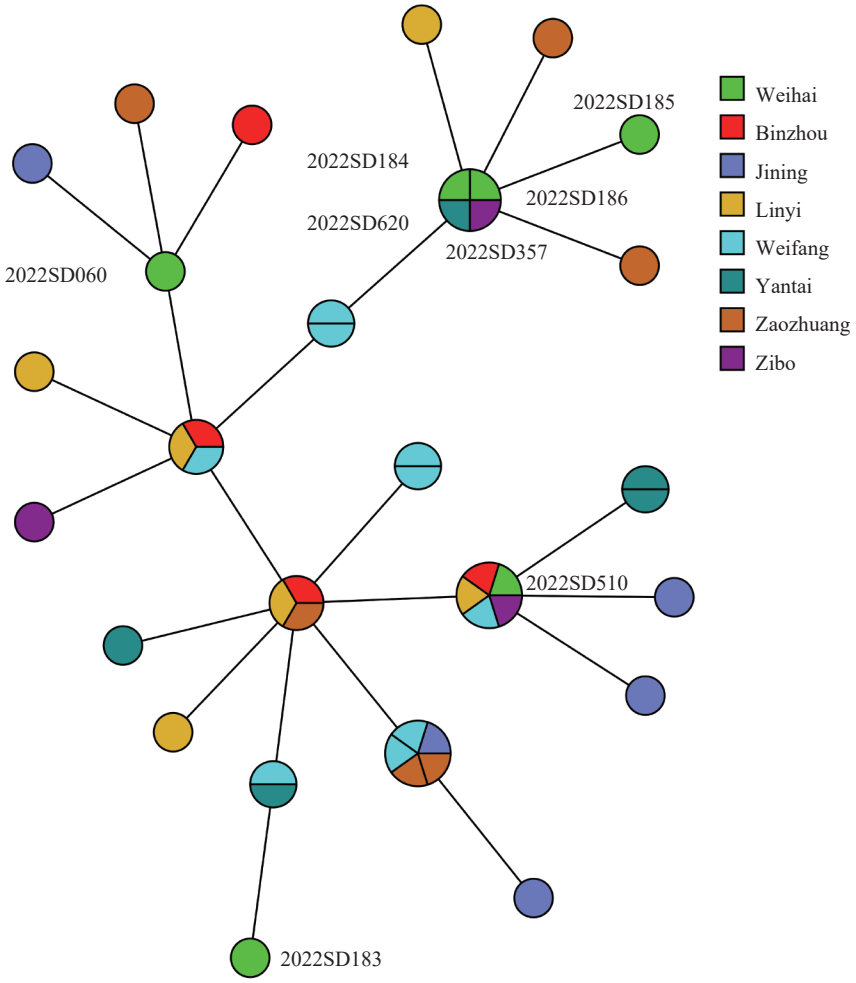

FIGURE 1. Minimum spanning tree for *Brucella melitensis* generated using MLVA-16 data with Weihai isolates (green) and representative entries from monitoring data for Shandong Province in 2022.

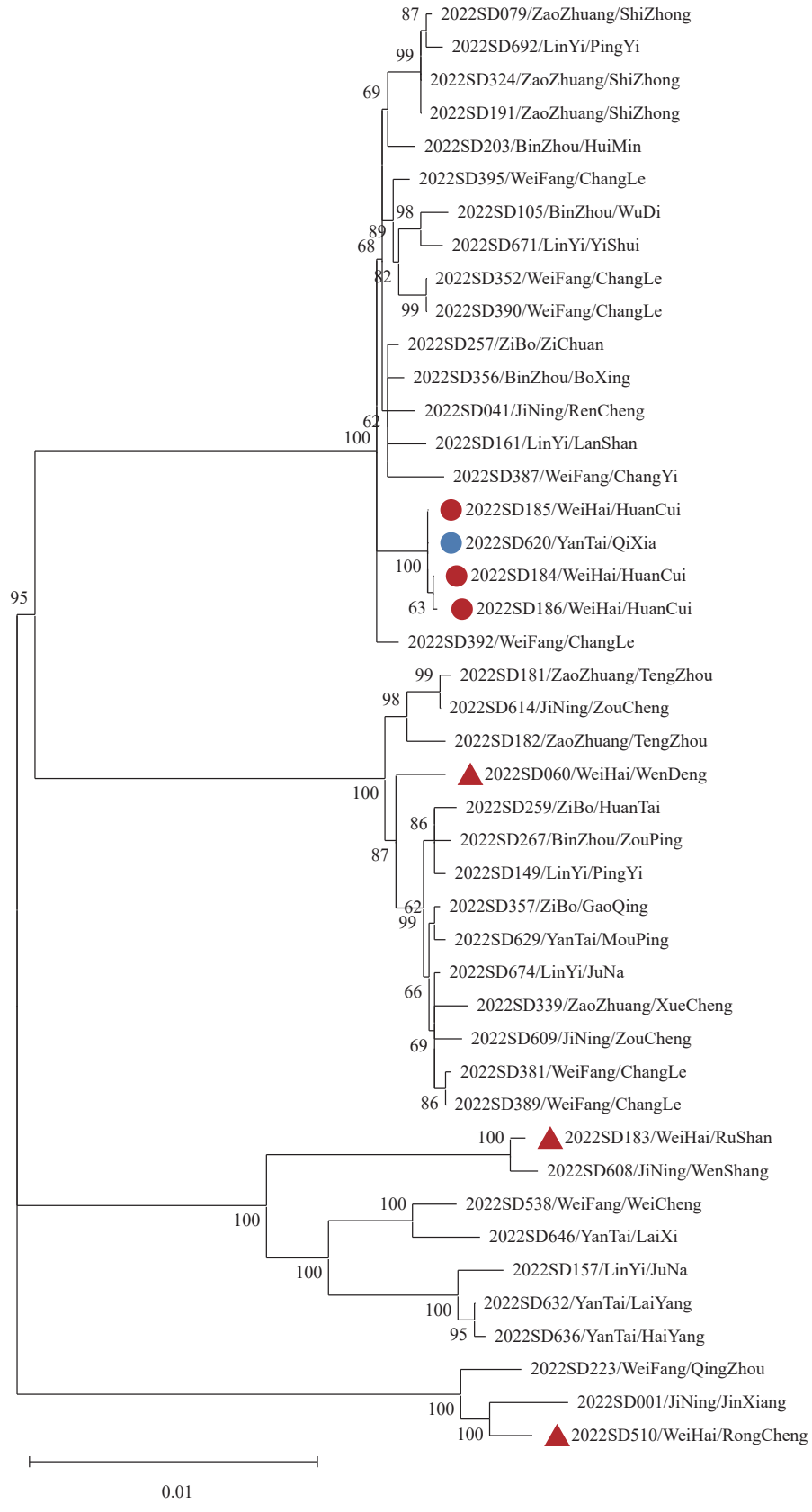

FIGURE 2. Neighbor-joining phylogenetic tree based on *Brucella melitensis* wgSNP types from Shandong Province.
Note: The red dots correspond to the strain in the outbreak, and the blue dots correspond to the outbreak-associated strain from Yantai City. The red triangles represent sporadic strains from Weihai City.

Additionally, a divergence of over 140 SNP loci was observed between the sporadic strains and the outbreak strains, indicating no evidence of transmission linkage, which aligns with the results obtained from MLVA-16 typing analyses (Figure 2). An advanced stratification analysis technique determined that the strain identified as B2022SD620, originating from Qixia City in Yantai, was identical to the strain associated with the current outbreak. By integrating epidemiological data and the geographic distribution of homologous strains, it was inferred that the spread of the epidemic likely resulted from trans-regional trade of contaminated livestock.

DISCUSSION

The prevalence of brucellosis in Shandong Province has seen a declining trend since its peak in 2016. However, there has been a notable resurgence of the disease since 2021. This resurgence has been largely attributed to the growth of the livestock breeding industry and increased interprovincial transport of livestock. The complexity and often clandestine nature of livestock trade, coupled with insufficient financial incentives for culling infected animals, have complicated the tracking of infection sources and destinations via epidemiological research. Our investigations revealed that in August 2021, patients had acquired sheep with unverified immunization and health statuses from Rushan, leading to subsequent infections during lambing and the handling of by-products. The substantial lapse of time between the initial outbreak and the acquisition of the infected sheep poses significant challenges to making headway in pinpointing the infection's origins through epidemiological methods.

The classical taxonomy of *B. melitensis*, based on biological species classification, sorts it into three biovars, yielding limited epidemiological insight due to poor resolution among isolates. In addition, the typing identification method based on bacterial culture has a large risk of biosafety, and the judgment of experimental results has a certain subjectivity.

MLVA is considered highly effective for *Brucella* spp. typing, reputed for its discriminating resolution (*4*). Yet, the MLVA-16 method produced inconsistent results for three strains from a recent outbreak. This suggests MLVA-16's limitation in providing precise resolution, predicting strains in long-term outbreaks, or establishing connections between strains without direct links over extended periods (*3*,*5*). To enhance the investigation's discriminatory capability, we examined 44 genome assemblies using a wgSNP approach, setting a 7-SNP threshold to identify a cluster of related cases. This analysis revealed a strain from Yantai Penglai clustering with strains from Weihai related to the outbreak, whereas other strains sharing the same MLVA type did not. The strains from Weihai were highly homologous to those from Yantai, suggesting frequent livestock movement between the cities. Although wgSNP analysis appears to provide superior discriminatory power among available typing methods, it lacks standardized procedures and is influenced by various factors, including nucleic acid extraction, library preparation, sequencing techniques, and bioinformatics analysis methods.

In conclusion, WGS data is valuable for enhancing insights into epidemiological dynamics, especially for source tracing during outbreaks involving zoonotic transmission and illegal animal movements. WGS data is more efficient than MLVA in assessing the potential for prolonged outbreaks and accurately predicting transmission routes (*6*).

Conflicts of interest: No conflicts of interest.

Funding: Supported by Medical and Health Development Plan of Shandong (2015WS0272), TCM science and technology project of Shandong (Q-2022091).

doi: 10.46234/ccdcw2024.046

[#] Corresponding author: Zengqiang Kou, jack-cou@163.com.

[1] Shandong Provincial Center for Disease Control and Prevention, Jinan City, Shandong Province, China; [2] Shandong First Medical University, Shandong Academy of Medical Sciences, Jinan City, Shandong Province, China; [3] Weihai Municipal Center for Disease Control and Prevention, Weihai City, Shandong Province, China.
[&] Joint first authors.

Submitted: December 11, 2023; Accepted: March 17, 2024

REFERENCES

1. Liu ZG, Wang M, Ta N, Fang MG, Mi JC, Yu RP, et al. Seroprevalence of human brucellosis and molecular characteristics of *Brucella* strains in Inner Mongolia Autonomous region of China, from 2012 to 2016. Emerg Microbes Infect 2020;9(1):263 – 74. https://doi.org/10.1080/22221751.2020.1720528.
2. Le Flèche P, Jacques I, Grayon M, Al Dahouk S, Bouchon P, Denoeud F, et al. Evaluation and selection of tandem repeat loci for a *Brucella* MLVA typing assay. BMC Microbiol 2006;6:9. https://doi.org/10.1186/1471-2180-6-9.
3. Janowicz A, De Massis F, Ancora M, Cammà C, Patavino C, Battisti A, et al. Core genome multilocus sequence typing and single nucleotide polymorphism analysis in the epidemiology of *Brucella melitensis* infections. J Clin Microbiol 2018;56(9):e00517 – 18. https://doi.org/10.1128/JCM.00517-18.

4. Carriço JA, Sabat AJ, Friedrich AW, Ramirez M, ESCMID Study Group for Epidemiological Markers (ESGEM). Bioinformatics in bacterial molecular epidemiology and public health: databases, tools and the next-generation sequencing revolution. Euro Surveill 2013;18(4):20382. https://doi.org/10.2807/ese.18.04.20382-en.
5. Zhu X, Zhao ZZ, Ma SY, Guo ZW, Wang M, Li ZJ, et al. *Brucella melitensis*, a latent "travel bacterium," continual spread and expansion from Northern to Southern China and its relationship to worldwide lineages. Emerg Microbes Infect 2020;9(1):1618 – 27. https://doi.org/10.1080/22221751.2020.1788995.
6. Kamath PL, Foster JT, Drees KP, Luikart G, Quance C, Anderson NJ, et al. Genomics reveals historic and contemporary transmission dynamics of a bacterial disease among wildlife and livestock. Nat Commun 2016;7:11448. https://doi.org/10.1038/ncomms11448.

Vital Surveillances

Epidemiological Characteristics of Human Parainfluenza Viruses Infections — China, 2019–2023

Yixuan Gao[1]; Yingwei Ma[2]; Daxing Feng[3]; Feng Zhang[4]; Biao Wang[5]; Xiaoqing Liu[6]; Bing Zhu[7]; Hui Xie[8]; Linqing Zhao[9]; Xiaoru Long[10]; Ying Chen[11]; Bing Wang[12]; Jie Jiang[1]; Zhen Zhu[1]; Yan Zhang[1]; Aili Cui[1]; Baicheng Xia[1]; Naiying Mao[1,#]

ABSTRACT

Introduction: A retrospective study based on sentinel surveillance was conducted in 10 provincial-level administrative divisions (PLADs) in China to enhance the understanding of the epidemiological characteristics of human parainfluenza viruses (HPIVs).

Methods: From January 2019 to June 2023, respiratory specimens were collected from individuals with acute respiratory infections (ARIs) and screened for four HPIVs serotypes and other common respiratory viruses using multiplex real-time polymerase chain reaction (PCR). This study analyzed the association of HPIVs infections with seasonal patterns, geographical distribution, demographic profiles, clinical features, and co-infection status.

Results: During the study period, a total of 12,866 ARIs were included. The overall detection rate of HPIVs was 6.15%, varying from 5.04% in 2022 to 9.70% in 2020. The median age of HPIVs-infected patients was 3 years. HPIV2 was more prevalent among individuals aged 5–17 years (42.57%), while HPIV4 was more common in those over 65 years (12.24%). HPIV3 (54.16%) and HPIV1 (27.18%) were the predominant serotypes, and their prevalence exhibited significant seasonal fluctuations post-coronavirus disease 2019 (COVID-19) pandemic. The peak of HPIV3 shifted three months later in 2020 compared to 2019 and returned to a summer peak thereafter. Two peaks of HPIV1 were observed in 2021 following the peak of HPIV3. Additionally, co-infections were frequent in HPIVs cases (overall rate: 22.12%), with human rhinovirus being the most common co-infecting virus.

Conclusions: The prevalence of HPIVs in China was predominantly due to HPIV3 and HPIV1, and their seasonal patterns were altered by pandemic restrictions. Hence, continuous surveillance of HPIVs is essential.

Human parainfluenza viruses (HPIVs) are significant viral agents causing acute respiratory infections (ARIs) and severe acute respiratory infections (SARIs) in children globally (*1*–*3*). Currently, there are four known serotypes (HPIV1 to HPIV4) (*2*). HPIV1 and HPIV3 are more prevalent, with epidemics typically occurring in the fall and summer, respectively. In contrast, HPIV2 and HPIV4 are primarily active during the winter and spring months (*4*–*5*). The coronavirus disease 2019 (COVID-19) pandemic has led to observable seasonal changes in the patterns of several respiratory viruses (*6*–*7*). The objective of this study was to analyze epidemiological characteristics of HPIVs infections, aiming to offer a crucial scientific groundwork for preventing and controlling HPIVs epidemic in China.

METHODS

Clinical samples were collected from 11 sentinel sites across 10 provincial-level administrative divisions (PLADs), including seven PLADs in northern China (Beijing Municipality; Inner Mongolia Autonomous Region; and Henan, Gansu, Jilin, Liaoning, and Shandong provinces) and three PLADs in southern China (Chongqing Municipality, Jiangxi and Guangdong provinces). Following the case definitions in the guideline for hospitalized acute respiratory infections (ARIs) and severe acute respiratory infections (SARIs, 2011 version) released by the National Health Commision (*8*), a minimum of 20 ARIs patients per month were included in the study, with respiratory samples taken for pathogen screening. The study was approved by the Second Ethics Review Committee of the National Institute for Viral Disease Control and Prevention at China CDC, and informed consent was obtained from all patients or their

guardians before sample collection.

A commercial nucleic acid detection kit (Kinghawk, Beijing, China) was used to identify twelve viral respiratory pathogens, including HPIVs (HPIV1 to HPIV4), respiratory syncytial virus (HRSV), influenza virus (IFV), human adenovirus (HAdV), human rhinovirus (HRV), human metapneumovirus (HMPV), human enterovirus (HEV), human bocavirus (HBoV), and human coronavirus (HCoV). Prior to testing, all assays underwent validation.

Categorical data were analyzed using the chi-square (χ^2) test and Fisher's exact test, while continuous data were assessed using median tests. Statistical analyses were conducted using R (version 4.1.3, R Core Team and the R Foundation for Statistical Computing, Vienna, Austria). Statistical significance was defined as a P-value <0.05.

RESULTS

Overall Detection

During the study period, we enrolled 12,866 cases of ARIs. Excluding the 14.18% (1,825) of cases that lacked relevant clinical information, 70.46% (9,066) were classified as SARIs, while 15.35% (1,975) were considered mild ARIs. The median age of patients with ARIs was 3 years (range: 1 day to 100 years), and 71.34% were under the age of 5 years. A majority of the patients, 80.7% (10,378/12,866) hailed from northern PLADs (Table 1), with males accounting for 57.88%. The overall viral detection rate among the ARIs was 38.18% (4,912/12,866). HPIVs were identified in 6.15% (791/12,866) of the cases, being the third most frequently detected viruses following HRSV at 12.37% (1,592/12,866) and HRV at 9.44% (1,214/12,866). Within the HPIVs-positive ARIs, HPIV3 was the most common serotype, accounting for 54.61% (432/791), followed by HPIV1 at 27.18% (215/791), HPIV2 at 12.77% (101/791), and HPIV4 at 6.19% (49/791) (Table 1, Supplementary Table S1, available at https://weekly.chinacdc.cn/).

Out of 9,066 SARIs, the overall viral detection rate was 37.13% (3,366/9,066). The detection rates of HPIVs at 5.40% (490/9,066) in SARIs were in line with ARIs. Among HPIVs-infected individuals, HPIV3 was the most prevalent at 58.16% (285/490), followed by HPIV1 at 27.35% (134/490), HPIV2 at 8.98% (44/490), and HPIV4 at 5.92% (29/490) (Supplementary Table S2, available at https://weekly.chinacdc.cn/).

The detection rate of HPIVs among mild ARIs (6.84%, 135/1,975) was similar to that of all ARIs and SARIs. HPIV3 (40%, 54/135) was the most commonly detected type, while HPIV4 (5.93%, 8/135) was the least detected. Interestingly, in mild ARIs, HPIV2 (28.15%, 38/135) had a slightly higher prevalence than HPIV1 (25.96%, 35/135).

TABLE 1. Geographical distribution of HPIVs infections in China from 2019 to 2023.

PLADs	Period	No. of samples	Region of China	No. of HPIVs cases included in the analysis				
				HPIV1 (%)	HPIV2 (%)	HPIV3 (%)	HPIV4 (%)	HPIVs
Jilin	2019–2023	2,927	Northern	60 (43.5)	1 (0.7)	78 (56.5)	0 (0)	138*
Henan	2019–2022	2,068	Northern	24 (22.6)	22 (20.8)	45 (42.5)	15 (14.2)	106
Shandong	2019–2023	1,509	Northern	21 (18.2)	14 (12.1)	76 (66.0)	5 (4.3)	115†
Gansu	2020–2023	1,446	Northern	34 (23.1)	35 (23.8)	66 (44.9)	12 (8.2)	147
Beijing	2019–2023	1,444	Northern	36 (36.7)	14 (14.3)	40 (40.8)	9 (9.2)	98†
Inner Mongolia	2021–2023	537	Northern	0 (0)	8 (21.6)	25 (67.6)	4 (10.8)	37
Liaoning	2021–2022	447	Northern	0 (0)	3 (60.0)	2 (40.0)	0 (0)	5
Jiangxi	2021–2023	1,069	Southern	4 (57.1)	0 (0)	3 (42.9)	1 (14.3)	7§
Guangdong	2021–2023	841	Southern	21 (31.3)	0 (0)	46 (68.7)	0 (0)	67
Chongqing	2020–2023	578	Southern	15 (21.1)	4 (5.6)	51 (71.8)	3 (4.2)	71*¶
Total	2019–2023	12,866	China	215 (27.2)	101 (12.8)	432 (54.6)	49 (6.2)	791

Note: Due to co-infection among the four HPIVs serotypes, the total number of cases counted in the table for the four serotypes was higher than the number of actual HPIVs infections.

Abbreviation: HPIVs=human parainfluenza viruses; PLADs=provincial-level administrative divisions.

* it included one case with HPIV1 and HPIV3 co-infection.

† it included one case with HPIV2 and HPIV4 co-infection.

§ it included one case with HPIV1 and HPIV4 co-infection.

¶ it included one case with HPIV3 and HPIV4 co-infection.

Season Pattern

The detection rate of HPIVs increased from 5.07% (78/1,539) in 2019 to 9.70% (146/1,505) in 2020, decreased to 7.63% (311/4,075) in 2021, and further dropped to 5.04% (208/4,124) in 2022 (Figure 1, Supplementary Table S3, available at https://weekly.chinacdc.cn/). The epidemics of HPIV1 and HPIV3 exhibited distinct seasonal patterns.

The incidence of HPIV1 showed a peak between August and December 2019, then shifted to the winter period from December 2020 to January 2021. Subsequently, two peaks were observed in July and October 2021. In 2021, the detection rate of HPIV1 was highest at 3.46% (141/4,075) (P<0.001) (Supplementary Table S3). However, from January 2022 to June 2023, the detection of HPIV1 decreased, maintaining a relatively low level at 0.51% and 0.37% without a distinct peak (Figure 1).

The incidence of HPIV3 differed from HPIV1, peaking in summer (June–August) in 2019, shifting to autumn and winter (October–November) in 2020, and returning to summer (June–August) in 2021 and 2022.

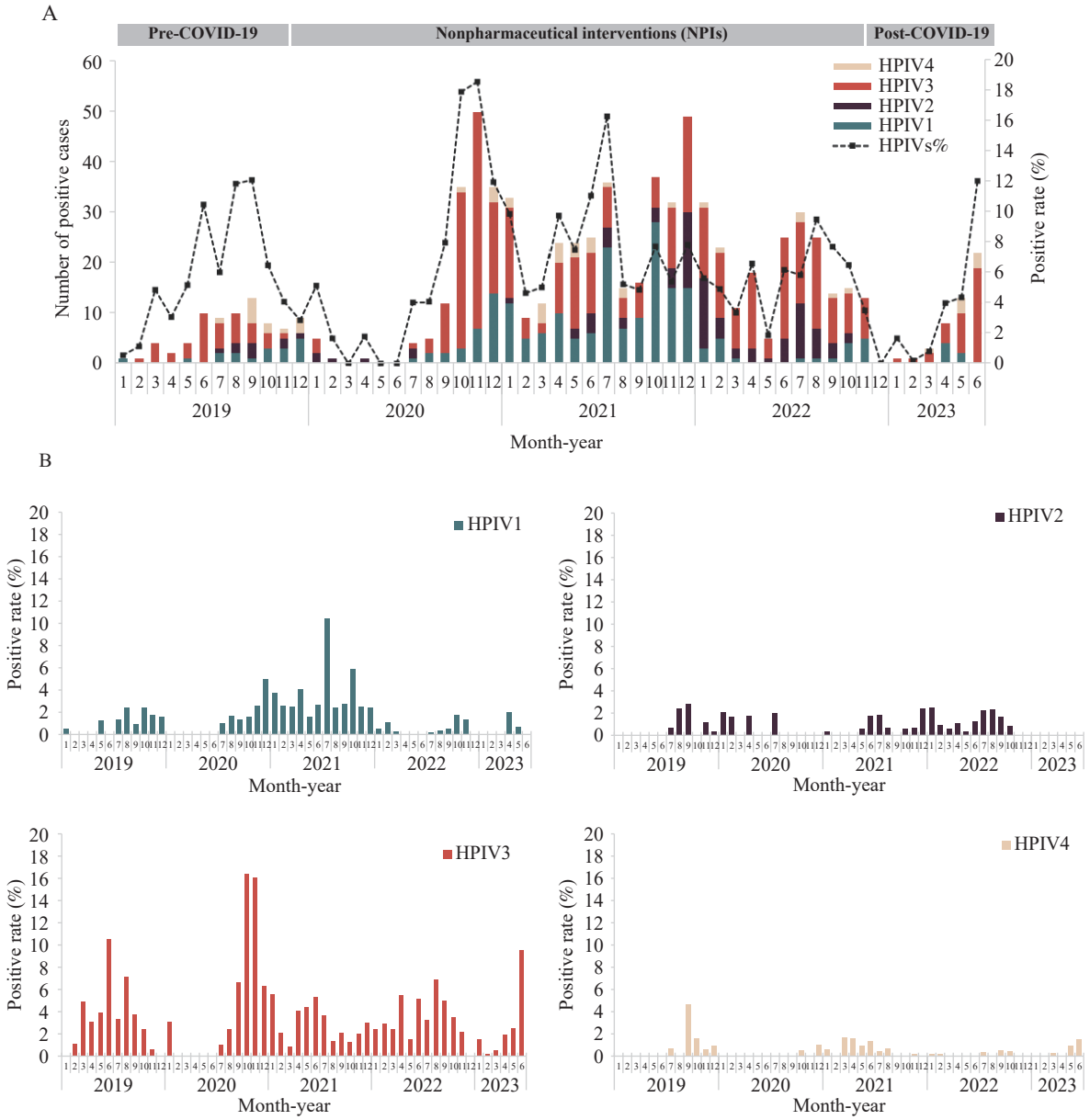

FIGURE 1. Season pattern of HPIVs in China from 2019 to 2023. (A) Detection of HPIVs by year. (B) Detection of HPIV1 to HPIV4 by year.
Abbreviation: HPIVs=human parainfluenza viruses; COVID-19=coronavirus disease 2019.

HPIV2 showed the highest detection rate in 2022 (1.24%, *P*=0.010) and was present all year except in November and December. In contrast, HPIV4 was only sporadically detected, with a higher rate in 2019 (0.78%, *P*=0.002) (Supplementary Table S3). There was no significant seasonal pattern observed for these two serotypes (Figure 1).

Geographical Distribution

The prevalence of HPIVs serotypes varied across different PLADs as shown in Table 1. HPIV1 and HPIV3 were the most common in northern and southern China, especially HPIV3 which had a higher prevalence in southern regions (4.02%, 100/2,488) compared to northern regions (3.20%, 332/10,378) (*P*<0.001). Conversely, the detection rates of HPIV2 (0.93%, 97/10,378) and HPIV4 (0.43%, 45/10,378) were higher in northern PLADs than in the southern PLADs (*P*<0.001, *P*=0.047) (Supplementary Table S3).

Demographic Profile

Among the 791 patients infected with HPIVs, 59.29% were male, with no sex-based difference observed (Table 2). The median age of the patients was 3 years, ranging from 1 month to 90 years, with the majority being children under 5 years old (77.24%), followed by individuals aged 5–17 years (16.69%) and those aged 65 years and older (3.92%)(Table 2). Notably, a significant difference was found in the age distribution for HPIV2 and HPIV4 infections (*P*<0.001). HPIV2 was more prevalent in the 5-17 years age group (42.57%), while HPIV4 was predominant in those over 65 years old (12.24%) (Table 2). Moreover, there were no significant variations in sex, age, or region for mono- and co-infections of HPIVs (Supplementary Table S4, available at https://weekly.chinacdc.cn/).

In 490 SARIs caused by HPIVs, the median age was 2 years (range: 1 month to 90 years). The gender and age distributions of HPIVs infections among SARIs were similar to those in ARIs (Supplementary Table S5, available at https://weekly.chinacdc.cn/).

Clinical Features

The analysis included 6,442 ARIs with complete clinical information, of which 357 cases were HPIVs infections. The symptoms manifested by HPIVs patients included fever (87.39%, *P*=0.002), cough (83.47%, *P*=0.023), phlegm production (49.86%, *P*<0.001), sore throat (33.33%, *P*<0.001), headache (14.57%, *P*<0.001), and diarrhea (7.28%, *P*=0.013) (Table 3). HPIV2-infected patients were particularly more likely to experience fever (97.73%, *P*=0.024), produce phlegm (72.73%, *P*<0.001), headaches (65.91%, *P*<0.001), and sore throats (54.55%, *P*=0.008). Rhinorrhea was notably seen in HPIV4 infections (75%, *P*<0.001), although this observation could be influenced by the limited number of HPIV4 cases within the study (Table 3). Additionally, co-infection with HPIVs was associated with a higher incidence of headache symptoms (33.33%), which was higher than that in patients with HPIVs mono-infection (0.97%, *P*<0.001)(Table 3).

Among the 278 SARIs caused by HPIVs, common symptoms were "cough" (88.85%, *P*=0.001), "rhinorrhea" (44.24%, *P*=0.007), and "diarrhea"

TABLE 2. Demographic characteristics of HPIVs infections among patients with ARIs (January 2019–June 2023).

Characteristic	HPIV1 *n*=215	HPIV2 *n*=101	HPIV3 *n*=432	HPIV4 *n*=49	*P*	HPIVs *n*=791
M (Q_1, Q_3)	3 (1, 4)	4 (3, 6)	2 (1, 3)	3 (2, 5)	<0.001	3 (1, 4)
Age (years), *N* (%)					<0.001	
0–4	169 (78.60)	52 (51.49)	361 (83.56)	33 (67.35)		611 (77.24)
5–17	30 (13.95)	43 (42.57)	52 (12.04)	8 (16.33)		132 (16.69)
18–39	1 (0.47)	0 (0)	1 (0.23)	1 (2.04)		3 (0.38)
40–64	3 (1.40)	2 (1.98)	8 (1.85)	1 (2.04)		14 (1.77)
65+	12 (5.58)	4 (3.96)	10 (2.31)	6 (12.24)		31 (3.92)
Sex, *N* (%)					0.746	
Male	121 (56.28)	59 (58.42)	262 (60.65)	30 (61.22)		469 (59.29)
Female	94 (43.72)	42 (41.58)	170 (39.35)	19 (38.78)		322 (40.71)

Abbreviation: HPIVs=human parainfluenza viruses; ARIs=acute respiratory infections.

(9.35%, *P*=0.010). Conversely, non-SARIs were more likely to experience symptoms such as "fever" (96.20%, *P*=0.013), "phlegm" (69.62%, *P*=0.001), "headache" (56.96%, *P*=0.010), or "sore throat" (51.90%, *P*=0.001) (Supplementary Table S6, available at https://weekly.chinacdc.cn/).

Co-Infection Status

Co-infection was frequent in HPIVs infections, with co-infection rate of 22.12% (175/791). Dual co-infections were the most common (132/175, 75.43%), followed by triple co-infections (26/175, 14.86%) and quadruple or higher co-infections (17/175, 9.71%). The top three pathogens co-infected with HPIVs were HRV (69/791, 8.72%), HRSV (43/791, 5.44%), and HAdV (40/791, 5.06%). However, the rates of co-infection between HPIVs and associated viruses varied by year (*P*=0.04). The highest co-infection rate with HPIVs was in 2019 (25/78, 32.05%), with HCoV (9/25, 36%) being the most common co-infected virus. The lowest co-infection rate was in 2020 (26/146, 17.81%), with HAdV (10/26, 38.46%) as the predominant co-infected virus. HRV was the primary co-infected virus in 2021 (26/60, 43.33%) and 2022 (25/49, 51.02%). During January–June 2023, both HRV (5/15, 33.33%) and IFV (5/15, 33.33%) were the major co-infected viruses (Table 4).

The co-infection rate among SARIs caused by HPIVs was 26.9% (132/490), which was not different from ARIs (*P*=0.050). Dual co-infections were predominant in HPIVs-related infections.

The most common viruses co-infected with HPIVs in ARIs, SARIs, and mild ARIs were HRV, HRSV, and HADV. The association between combined viral infections and increased disease severity was not observed.

TABLE 3. Clinical characteristics of HPIVs infections.

Symptoms	HPIVs infection in 6,442 ARIs			4 types of distribution in 357 HPIVs-positive ARIs					HPIVs infections status		
	HPIVs-positive (*n*=357)	HPIVs-negative (*n*=6,085)	*P*	HPIV1 (*n*=108)	HPIV2 (*n*=44)	HPIV3 (*n*=197)	HPIV4 (*n*=8)	*P*	Mono-HPIVs (*n*=207)	Co-pathogens (*n*=150)	*P*
Fever	312 (87.39)	4,904 (80.59)	0.002	98 (90.74)	43 (97.73)	164 (83.25)	7 (87.50)	0.024	175 (84.54)	137 (91.33)	0.081
Cough	298 (83.47)	4,762 (78.26)	0.023	90 (83.33)	32 (72.73)	169 (85.79)	7 (87.50)	0.204	180 (86.96)	118 (78.67)	0.053
Sore throat	119 (33.33)	1,243 (20.43)	<0.001	30 (27.78)	24 (54.55)	61 (30.96)	4 (50.00)	0.008	60 (28.99)	59 (39.33)	0.053
Rhinorrhoea	114 (31.93)	2,128 (34.97)	0.045	30 (27.78)	14 (31.82)	94 (47.72)	6 (75.00)	<0.001	80 (38.65)	64 (42.67)	0.513
Phlegm	178 (49.86)	2,410 (39.61)	<0.001	64 (59.26)	32 (72.73)	79 (40.10)	3 (37.50)	<0.001	95 (45.89)	83 (55.33)	0.098
Chest pain	2 (0.56)	70 (1.15)	0.437	0 (0)	1 (2.27)	1 (0.51)	0 (0)	0.361	2 (0.97)	0 (0)	0.511
Dyspnea	19 (5.32)	416 (6.84)	0.317	5 (4.63)	3 (6.82)	10 (5.08)	1 (12.50)	0.570	12 (5.80)	7 (4.67)	0.818
Headache	52 (14.57)	437 (7.18)	<0.001	15 (13.89)	29 (65.91)	7 (3.55)	1 (12.50)	<0.001	2 (0.97)	50 (33.33)	<0.001
Abdominal pain	12 (3.36)	195 (3.20)	0.993	5 (4.63)	1 (2.27)	5 (2.54)	1 (12.50)	0.281	8 (3.86)	4 (2.67)	0.747
Diarrhea	26 (7.28)	263 (4.32)	0.013	4 (3.70)	1 (2.27)	21 (10.66)	0 (0.00)	0.074	13 (6.28)	13 (8.67)	0.516

Abbreviation: HPIVs=human parainfluenza viruses; ARIs=acute respiratory infections.

TABLE 4. Co-infection status of HPIVs infections in China from 2019 to 2023.

Time	HPIVs infections	8 respiratory viruses co-infected with HPIVs								Co-infection status		
		HRSV	HAdV	HRV	HMPV	HEV	HBoV	HCOV	IFV	Dual	Triple and more	Total [*n*, (%)]
2019	78	0	6	7	1	6	2	9*	1	19	6	25 (32.05)
2020	146	5	10*	6	1	7	6	4	1	17	9	26 (17.81)
2021	311	24	13	26*	4	13	13	0	1	43	17	60 (19.29)
2022	208	11	9	25*	3	4	3	2	8	40	9	49 (23.56)
2023 (Jan–Jun)	48	3	2	5*	0	0	2	0	5*	13	2	15 (31.25)
Total	791	43	40	69*	9	30	26	15	16	132	43	175 (22.12)

Abbreviation: HPIVs=human parainfluenza viruses; HRSV=respiratory syncytial virus; HAdV=human adenovirus; HRV=humanrhinovirus; HMPV=human metapneumovirus; HEV=human enterovirus; HBoV=humanbocavirus; HCoV=human coronavirus; IFV=influenzavirus.
* represents the most common co-infected virus per year.

CONCLUSION

The recent surge of ARIs in children within China has garnered international concern (*9*), epidemic trends of HPIVs were examined in this study. The current analysis found an overall HPIVs detection rate of 6.15% in ARIs and 5.40% in SARIs, aligning with the results of earlier research (*10*–*11*). HPIVs ranked third among the most commonly identified respiratory pathogens, following HRSV and HRV. Among four HPIVs serotypes, HPIV3 and HPIV1 were the most frequently observed strains, suggesting these two serotypes chiefly influence HPIVs epidemiology in China. Interestingly, the study also noted HPIV2 as prevalent in mild ARIs, a finding which warrants further verification. Additionally, nonpharmacological interventions (NPIs) might influence HPIVs epidemic patterns. Notably, fewer HPIVs infections were recorded in the first half of 2020; however, cases surged in the latter half of the year following the easing of NPIs.

This study identified notable alterations in the seasonal patterns of HPIV3 and HPIV1 following the COVID-19 pandemic. Specifically, the 2020 epidemic peak for HPIV3 shifted to the autumn and winter months, a three-month postponement from its usual summer peak observed in 2019. Post-2020, HPIV3 levels stabilized. In 2021, two successive epidemic peaks of HPIV1 were recorded in July and October, which directly succeeded the peak of HPIV3. A comparable delay in HPIVs seasonal peaks has been documented in South Africa post-pandemic (*12*). These timing shifts may be attributed to the enactment of NPIs, changes in societal behaviors, and the presence of immunity gaps among the population. No conspicuous seasonal trends were identified for HPIV2 and HPIV4, and their epidemiological patterns remain largely undefined within China, underscoring the imperative for ongoing monitoring.

Although co-infections with HPIVs were common, their incidence varied annually, peaking at 32.05% in 2019 and dropping to 17.81% in 2020. The decrease may be attributed to the reduced presence of common co-infecting viruses due to NPIs. HRV was frequently identified as a co-infecting agent, showing a positive correlation with HPIVs (*13*). The high occurrence of HPIVs and HRV co-infections could be linked to their transmission modes via direct contact, which might have been facilitated by lower adherence to preventive measures during NPIs. The co-infection rate of HPIVs rose significantly following the relaxation of NPIs. Given that co-infections often lead to severe conditions (*14*), the significance of addressing co-infections in HPIVs cases should be underscored.

HPIVs are distinguished by their infection age, clinical manifestations, and geographic prevalence (*15*). This study found that HPIVs predominantly infected children under five years old. However, HPIV2 was more frequently diagnosed in both children and adolescents, whereas HPIV4 was often detected in the elderly, confirming earlier reports (*12*). Furthermore, although HPIVs infections are known to cause a broad spectrum of clinical symptoms, certain serotype-specific manifestations such as fever, phlegm, and headache have been particularly associated with HPIV2 infections. The distribution of HPIVs across China also exhibited regional variability; for instance, HPIV3 was more commonly found in the southern PLADs, whereas HPIV2 and HPIV4 showed higher occurrences in the northern areas. Nevertheless, these observed serotype-specific epidemiological trends necessitate corroboration through extended surveillance data.

In conclusion, analysis of five years of surveillance data has unveiled the epidemic patterns of HPIVs in China. This has enhanced comprehension of the epidemiological and clinical features of HPIVs and has implications for the prevention and management of HPIVs-related respiratory diseases in China.

Conflicts of interest: No conflicts of interest.

Funding: Supported by the National Health Commission Major Public Health Project (ZDGW21-131031103000180005).

doi: 10.46234/ccdcw2024.047

[#] Corresponding author: Naiying Mao, maony@ivdc.chinacdc.cn.

[1] National Key Laboratory of Intelligent Tracking and Forecasting for Infectious Diseases, National Institute for Viral Disease Control and Prevention, Chinese Center for Disease Control and Prevention; Beijing, China; [2] Precision Medicine Research Center, Children's Hospital of Changchun, Changchun City, Jilin Province, China; [3] Henan Provincial Center for Disease Control and Prevention, Zhengzhou City, Henan Province, China; [4] Laboratory of Viral Diseases, Qingdao Municipal Centre for Disease Control and Prevention, Qingdao City, Shandong Province, China; [5] Virus Laboratory, Gansu Provincial Center for Disease Control and Prevention, Lanzhou City, Gansu Province, China; [6] Jiangxi Provincial Center for Disease Control and Prevention, Nanchang City, Gansu Province, China; [7] Virus Laboratory, Guangzhou Women and Children's Medical Center, Guangzhou Medical University, Guangzhou City, Guangdong Province, China; [8] Institute for Immunization and Prevention, Beijing Center for Disease Prevention and Control, Academy for Preventive Medicine, Institute of Tuberculosis Control Research and Prevention, Beijing, China; [9] Laboratory of Virology, Beijing Key Laboratory of Etiology of Viral Diseases in Children, Capital Institute of Pediatrics, Beijing, China; [10] Department of Infection, Children's Hospital of Chongqing Medical

University, Chongqing, China; [11] Inner Mongolia Autonomous Region Comprehensive Center for Disease Control and Prevention, Hohhot City, Inner Mongolia Autonomous Region, China; [12] Shenyang Prefecture Center for Disease Control and Prevention, Shenyang City, Liaoning Province, China.

Submitted: September 11, 2023; Accepted: March 17, 2024

REFERENCES

1. Wang X, Li Y, Deloria-Knoll M, Madhi SA, Cohen C, Arguelles VL, et al. Global burden of acute lower respiratory infection associated with human parainfluenza virus in children younger than 5 years for 2018: a systematic review and meta-analysis. Lancet Glob Health 2021;9(8): e1077 – 87. https://doi.org/10.1016/s2214-109x(21)00218-7.
2. Branche AR, Falsey AR. Parainfluenza virus infection. Semin Respir Crit Care Med 2016;37(4):538 – 54. https://doi.org/10.1055/s-0036-1584798.
3. Gregianini TS, Seadi CF, Zavarize Neto LD, Martins LG, Muller GC, Straliotto SM, et al. A 28-year study of human parainfluenza in Rio Grande do Sul, Southern Brazil. J Med Virol 2019;91(8):1423 – 31. https://doi.org/10.1002/jmv.25459.
4. Liu WK, Liu Q, Chen DH, Liang HX, Chen XK, Huang WB, et al. Epidemiology and clinical presentation of the four human parainfluenza virus types. BMC Infect Dis 2013;13:28. https://doi.org/10.1186/1471-2334-13-28.
5. DeGroote NP, Haynes AK, Taylor C, Killerby ME, Dahl RM, Mustaquim D, et al. Human parainfluenza virus circulation, United States, 2011-2019. J Clin Virol 2020;124:104261. https://doi.org/10.1016/j.jcv.2020.104261.
6. Olsen SJ, Azziz-Baumgartner E, Budd AP, Brammer L, Sullivan S, Pineda RF, et al. Decreased influenza activity during the COVID-19 pandemic-United States, Australia, Chile, and South Africa, 2020. Am J Transplant 2020;20(12):3681 – 5. https://doi.org/10.1111/ajt.16381.
7. Wang L, Berger N, Davis PB, Kaelber DC, Volkow N, Xu R. Time trend and seasonality in medically attended respiratory syncytial virus (RSV) infections in US children aged 0–5 years, January 2010–January 2023. Fam Med Community Health 2023;11(4):e002453. https://doi.org/10.1136/fmch-2023-002453.
8. National Health Commision. Guideline for Sentinel Surveillance of Hospitalized SARIs cases (2011 version). 2011. http://www.nhc.gov.cn/jkj/s3577/201102/cf5a16a948ef45198281e6334f7dfbd8.shtml [2011-2-11]. (In Chinese).
9. World Health Organization. Upsurge of respiratory illnesses among children-Northern China. 2023. https://www.who.int/emergencies/disease-outbreak-news/item/2023-DON494. [2023-11-23].
10. Li X, Liu XW, Zhou T, Pei XF. Detection and analysis of human parainfluenza virus infection in hospitalized adults with acute respiratory tract infections. J Sichuan Univ (Med Sci) 2017;48(6):891 – 4. https://doi.org/10.13464/j.scuxbyxb.2017.06.019.
11. Xie H, Luo M, Huang Q, Li AH, Wang X, Gong C, et al. Epidemiology of human parainfluenza virus infection in patients with acute respiratory tract infection in Beijing, 2015-2020. Dis Surveill 2021;36(9):943 – 8. https://doi.org/10.3784/jbjc.202104220219.
12. Parsons J, Korsman S, Smuts H, Hsiao NY, Valley-Omar Z, Gelderbloem T, et al. Human parainfluenza virus (HPIV) detection in hospitalized children with acute respiratory tract infection in the western cape, South Africa during 2014-2022 reveals a shift in dominance of HPIV 3 and 4 infections. Diagnostics 2023;13(15):2576. https://doi.org/10.3390/diagnostics13152576.
13. Madewell ZJ, Wang LP, Dean NE, Zhang HY, Wang YF, Zhang XA, et al. Interactions among acute respiratory viruses in Beijing, Chongqing, Guangzhou, and Shanghai, China, 2009-2019. Influenza Other Respir Viruses 2023;17(11):e13212. https://doi.org/10.1111/irv.13212.
14. Jain S, Self WH, Wunderink RG, Fakhran S, Balk R, Bramley AM, et al. Community-acquired pneumonia requiring hospitalization among U. S. adults. N Engl J Med 2015;373(5):415 – 27. https://doi.org/10.1056/NEJMoa1500245.
15. Farahmand M, Shatizadeh Malekshahi S, Jabbari MR, Shayestehpour M. The landscape of extrapulmonary manifestations of human parainfluenza viruses: a systematic narrative review. Microbiol Immunol 2021;65(1):1 – 9. https://doi.org/10.1111/1348-0421.12865.

SUPPLEMENTARY MATERIAL

SUPPLEMENTARY TABLE S1. The population distribution by age and sex among ARIs with HPIV1–HPIV4 infections from January 2019 to June 2023.

Characteristic	HPIV1 *n*=215	HPIV2 *n*=101	HPIV3 *n*=432	HPIV4 *n*=49	HPIVs *n*=791
Age (years), *N* (%)					
0–4	169 (27.66)	52 (8.51)	361 (59.08)	33 (5.40)	611
5–17	30 (22.72)	43 (32.57)	52 (39.39)	8 (6.06)	132
18–39	1 (33.33)	0 (0)	1 (33.33)	1 (33.33)	3
40–64	3 (21.42)	2 (14.29)	8 (57.14)	1 (7.14)	14
65+	12 (38.71)	4 (12.90)	10 (32.25)	6 (19.35)	31
Sex, *N* (%)					
Male	121 (25.80)	59 (12.58)	262 (55.86)	30 (6.39)	469
Female	94 (29.19)	42 (13.04)	170 (52.80)	19 (5.90)	322

Note: % is the ratio of the composition of the rows.
Abbreviation: HPIVs=human parainfluenza viruses; ARIs=acute respiratory infections.

SUPPLEMENTARY TABLE S2. The population distribution by age and sex among patients with SARIs caused by HPIV1 to HPIV4, from January 2019 to June 2023.

Characteristic	HPIV1 *n*=134	HPIV2 *n*=44	HPIV3 *n*=285	HPIV4 *n*=32	HPIVs *n*=490
Age (years), *N* (%)					
0–4	109 (26.98)	26 (6.44)	252 (62.38)	21 (5.20)	404
5–17	13 (27.08)	13 (27.08)	17 (35.42)	5 (10.42)	48
18–39	0 (0)	0 (0)	0 (0)	0 (0)	0
40–64	1 (9.09)	2 (18.18)	7 (63.64)	1 (9.09)	11
65+	11 (40.74)	3 (11.11)	9 (33.33)	5 (18.52)	27
Sex, *N* (%)					
Male	74 (25.52)	28 (9.66)	171 (58.97)	19 (6.55)	290
Female	60 (0.30)	16 (0.08)	114 (0.57)	13 (0.07)	200

Note: % is the ratio of the composition of the rows.
Abbreviation: HPIVs=human parainfluenza viruses; SARIs=severe acute respiratory infections.

SUPPLEMENTARY TABLE S3. Geographic distribution and annual detection positive rate of HPIVs.

Characteristic	HPIV1	HPIV2	HPIV3	HPIV4	HPIVs	ARIs
Region, *N* (%)						
Northern	175 (1.69)	97 (0.93)	332 (3.20)	45 (0.43)	646 (6.22)	10,378
Southern	40 (1.61)	4 (0.16)	100 (4.02)	4 (0.16)	145 (5.83)	2,488
P	0.784	<0.001	0.041	0.047	0.470	
Time, *N* (%)						
2019	18 (1.17)	9 (0.58)	39 (2.53)	12 (0.78)	78 (5.07)	1,539
2020	29 (1.93)	6 (0.40)	109 (7.24)	4 (0.27)	146 (9.70)	1,505
2021	141 (3.46)	35 (0.86)	116 (2.85)	20 (0.49)	311 (7.63)	4,075
2022	21 (0.51)	51 (1.24)	133 (3.23)	6 (0.15)	208 (5.04)	4,124
P	<0.001	0.010	<0.001	0.002	<0.001	

Note: % represents the positive detection rate (N/ARIs).
Abbreviation: HPIVs=human parainfluenza viruses; ARIs=acute respiratory infections.

SUPPLEMENTARY TABLE S4. Differences in the population distribution between HPIVs mono- and co-infections.

Characteristic	Mono-infections *n*=616	Co-infections *n*=175	*P*
M (Q_1, Q_3)	3 (1, 4)	2 (1, 4)	0.163
Age (years), *N* (%)			0.286
0–4	472 (76.62)	139 (79.43)	
5–17	102 (16.56)	30 (17.14)	
18–39	2 (0.32)	1 (0.57)	
40–64	14 (2.27)	0 (0)	
65+	26 (4.22)	5 (2.86)	
Sex, *N* (%)			0.515
Male	361 (58.60)	108 (61.71)	
Female	255 (41.40)	67 (38.29)	

Abbreviation: HPIVs=human parainfluenza viruses.

SUPPLEMENTARY TABLE S5. Demographics of HPIVs infections among SARIs (January 2019 to June 2023).

Characteristic	HPIV1 *n*=134	HPIV2 *n*=44	HPIV3 *n*=285	HPIV4 *n*=32	*P*	HPIVs *n*=490
M (Q_1, Q_3)	2 (1, 4)	4 (2.75, 7.25)	2 (0, 3)	3 (2, 5.25)	<0.001	2 (1, 3)
Age (years), *N* (%)					<0.001	
0–4	109 (81.34)	26 (59.09)	252 (88.42)	21 (65.63)		404 (82.45)
5–17	13 (9.70)	13 (29.55)	17 (5.96)	5 (15.63)		48 (9.80)
18–39	0 (0)	0 (0)	0 (0)	0 (0)		0 (0)
40–64	1 (0.75)	2 (4.55)	7 (2.46)	1 (3.13)		11 (2.24)
65+	11 (8.21)	3 (6.82)	9 (3.16)	5 (15.63)		27 (5.51)
Sex, *N* (%)					0.607	
Male	74 (55.22)	28 (63.64)	171 (60.00)	19 (59.38)		290 (59.18)
Female	60 (44.78)	16 (36.36)	114 (40.00)	13 (40.63)		200 (40.82)

Abbreviation: HPIVs=human parainfluenza viruses; SARIs=severe acute respiratory infections.

SUPPLEMENTARY TABLE S6. Clinical characteristics of HPIVs infections among patients with SARIs and non-SARIs.

Symptoms	357 HPIVs infections		*P*
	SARIs (*n*=278)	Non-SARIs (*n*=79)	
Fever	236 (84.89)	76 (96.20)	0.013
Cough	247 (88.85)	51 (64.56)	0.001
Sore throat	78 (28.06)	41 (51.90)	0.001
Rhinorrhea	123 (44.24)	21 (26.58)	0.007
Phlegm	123 (44.24)	55 (69.62)	0.001
Chest pain	2 (0.72)	0 (0)	0.053
Dyspnea	18 (6.47)	1 (1.27)	0.087
Headache	7 (2.52)	45 (56.96)	0.001
Abdominal pain	11 (3.96)	1 (1.27)	0.477
Diarrhea	26 (9.35)	0 (0)	0.010

Abbreviation: HPIVs=human parainfluenza viruses; SARIs=severe acute respiratory infections.

Outbreak Reports

An Outbreak of Serogroup Y Meningococcal Meningitis in a Private Secondary Vocational School — Guangzhou City, Guangdong Province, China, 2023

Xiang Zeng[1,2,3,&]; Qing He[4,&]; Yilan Li[4,5,&]; Yong Zhou[4]; Xiaoping Shao[3]; Pei Hu[3]; Jian Liang[3]; Yudan Song[6]; Chao Ma[6]; Lijie Zhang[1]; Limei Sun[3]; Lei Luo[4,#]

Summary

What is already known about this topic?

The inclusion of meningococcal vaccines in the National Immunization Program (NIP) over several years has significantly reduced the incidence of meningococcal meningitis in China to historic lows. Worldwide, there has been a diversification of meningococcal serogroups, leading to a shift in dominant serogroups in China from serogroup A to serogroups C and B, accompanied by a rise in reports of serogroups Y and W.

What is added by this report?

An outbreak of serogroup Y *Neisseria meningitidis (Nm)* in a secondary vocational school involved a single confirmed severe case and 24 individuals with laboratory-confirmed *Nm* carriage. Epidemiological investigation revealed that the outbreak was localized to the classroom of the confirmed case. Prolonged close contact within a confined space was identified as a significant risk factor for *Nm* transmission. The genotype sequence identified was type 1655 (ST-1655), which is categorized under clonal complex 23 (CC-23) and bears resemblance to 8 previously confirmed cases of serogroup Y meningococcal meningitis within Guangdong Province. This suggests that serogroup Y infections continue to sporadically emerge and have become prevalent strains.

What are the implications for public health practice?

This outbreak underscores the critical need to enhance surveillance of meningococcal serogroups and population carrier, and advocate for vaccination with MenY-containing vaccines.

At 2 p.m. on June 25, 2023, the Zengcheng District CDC reported to Guangzhou CDC that a blood sample from a severely ill child admitted to F Hospital for meningitis at F Hospital had tested positive for *Neisseria meningitidis* (*Nm*) via Metagenome Next Generation Sequencing (mNGS). The patient, a 16-year-old student from E School, prompted a collaborative effort between Guangdong CDC, Guangzhou CDC, and Zengcheng District CDC to conduct a comprehensive epidemiological field investigation. This investigation aimed to confirm the diagnosis, assess the extent, characteristics, and potential transmission risk factors of a suspected outbreak, and implement effective outbreak control measures.

INVESTIGATION AND RESULTS

E School is a private secondary vocational school situated in Zengcheng District, Guangzhou City. The matriculating class of 2022 comprises 1,847 students, as students from the 2020 and 2021 classes have departed for internships, with a total of 177 teachers and staff. The school operates as a closed boarding management institution with regular morning inspections and employs a full-time doctor. The school premises consist of repurposed old factories, situated in an industrial environment.

The confirmed case involved a male student residing in a school dormitory who had been previously healthy and had not received any MenY-containing vaccinations. As shown in Figure 1, symptoms began at 7 a.m. on June 23, manifesting as fever, headache, dizziness, and limb weakness. The individual took ibuprofen at noon and sought care at F Hospital's fever clinic at 8 p.m. Due to the rapid deterioration of his condition, he was promptly transferred to the emergency department at 9 p.m. and hospitalized in the ICU by 11 p.m. Progression of the illness was swift, characterized by lethargy, sepsis, shock, disseminated intravascular coagulation (DIC), multi-organ system failure, and widespread petechiae and ecchymosis — an indicative profile of fulminant meningococcal meningitis. Subsequent mNGS results from a blood sample taken on June 25 revealed the presence of an *Nm* sequence, with a serogroup Y

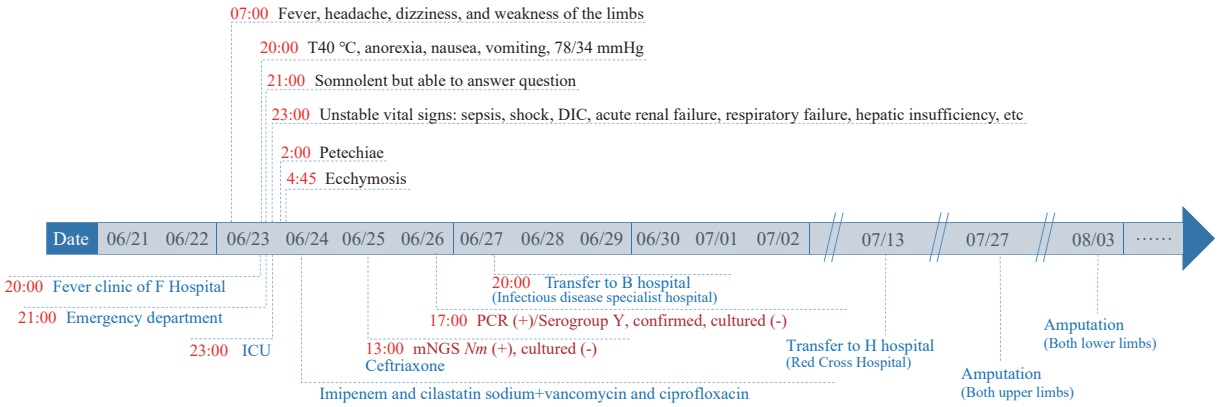

FIGURE 1. Timeline of symptoms, diagnosis, and treatment of the confirmed case.
Abbreviation: T=temperature; DIC=disseminated intravascular coagulation; ICU=intensive care unit; PCR=polymerase chain reaction; mNGS=metagenome next generation sequencing; *Nm=Neisseria meningitidis*.

meningococcal meningitis (fulminant) diagnosis confirmed on June 26 through positive *Nm* nucleic acid polymerase chain reaction (PCR) test results. Owing to dry necrosis in his limbs, surgical amputation was necessary. Following discharge from H Hospital on September 5, the patient transitioned to a local rehabilitation facility. Presently, he survives albeit with a compromised quality of life. Further details regarding the timeline, key symptoms, diagnosis, and management approaches can be observed in Figure 1.

A case definition was formulated, and a thorough case investigation was initiated to determine the extent of a potential outbreak. Following relevant national and provincial surveillance and diagnostic guidelines, a suspected case was characterized as an individual exhibiting fever, headache, vomiting, and/or meningeal irritation. This individual would either be associated with E school, residing in the school vicinity, or the surrounding community between June 1 and June 25, with no definitive exclusion of other diseases. A possible case was identified as a suspected case displaying skin (mucosal) petechiae and ecchymosis. A confirmed case was classified as a suspected or possible case where *Nm* was successfully cultured and isolated, or there was a positive result for *Nm* nucleic acid via PCR testing. A carrier was delineated as an individual with a positive *Nm* culture, or nucleic acid PCR result, but did not meet the criteria for a confirmed case. Close contacts were defined as individuals who had prolonged exposure to a confirmed case through shared living, educational, medical treatment, or dining settings.

Utilizing the specified case definitions, additional cases were sought through a comprehensive approach encompassing a review of school absence and medical records, interviews with various stakeholders including school administrators, doctors, classroom teachers, and classmates, along with scrutiny of medical records from two nearby healthcare facilities (F Hospital and a community health service center). No new confirmed, possible, or suspected cases were identified beyond the primary instance. A total of 82 close contacts were pinpointed, and throat swab samples were collected from them for *Nm* nucleic acid testing via PCR. Of these close contacts, 24 individuals (29.3%) tested PCR(+). Specifically, 23 were classmates of the index case, and one was the father of the index case. Among the 24 PCR(+) close contacts, 14 exhibited serogroup Y *Nm*, while the remaining ten were unclassified. A retrospective cohort study was conducted among the close contacts, revealing that the *Nm* nucleic acid PCR(+) rate was significantly higher among those who shared educational and living quarters with the confirmed case compared to other close contacts {46.0% *vs.* 3.1%, relative risk (RR): 14.7 [95% confidence interval (*CI*): 2.1, 103.7]}. Given the elevated carrier rate observed among the close contacts, a risk assessment was carried out by extending the sampling procedure to include the two classes adjacent to the index case's class, as well as individuals who dined in the school's cafeteria or engaged in activities such as sports with the confirmed case in outdoor areas, and individuals from surrounding factories and kindergartens. A total of 125 individuals were tested, all returning negative results. The testing outcomes for close contacts and other examined populations are detailed in Table 1 for reference.

We conducted an analysis of the seating arrangements among the 23 classmates who tested PCR(+). As depicted in Figure 2, groups that included the confirmed case or individuals who were roommates with the confirmed case showed higher rates of PCR(+) compared to groups without the confirmed case or his

TABLE 1. Sampling and detection of *Nm* nucleic acid PCR in close contacts and other populations.

Category	*N*	*Nm* nucleic acid PCR(+) *n* (%)	*Nm* serogroup
Close contact	82	24 (29.3)	14 Serogroup Y, 10 unclassified
Studied and lived in the same room	50	23 (46.0)	14 Serogroup Y, 9 unclassified
Learning in the same class	50	23 (46.0)	14 Serogroup Y, 9 unclassified
Living in the same dormitory	5*	3* (60.0)	Serogroup Y
Other close connection	32	1 (3.1)	Unclassified
Eating out together	3	0 (0)	–
Class teacher	9	0 (0)	–
Patient in the same ICU	16	0 (0)	–
Patient in the same emergency department	1	0 (0)	–
Family member	3	1† (33.3)	Unclassified
Expanded sample 1 — other people in the same school	80	0 (0)	–
Two adjacent classes	40	0 (0)	–
Dined in the canteen, played ball, etc.	40	0 (0)	–
Expanded sample 2 — outdoor activities places	15	0 (0)	–
Billiards club staff	4	0 (0)	–
Steak buffet restaurant staff	11	0 (0)	–
Expanded sampling 3 — factories and kindergartners around the school	30	0 (0)	–

Note: "–" means not applicable.
Abbreviation: PCR=polymerase chain reaction; ICU=intensive care unit; *Nm=Neisseria meningitidis*.
* Classmates of the confirmed case.
† Father of the confirmed case.

roommates (69.2% and 57.1% *vs.* 23.1% and 30.0%, respectively; $P<0.05$). Notably, the PCR(+) rates between Group 3, including the confirmed case, and Group 1, including the roommates of the confirmed case, did not exhibit a statistically significant difference (69.2% *vs.* 57.1%; $\chi^2=0.063$, $P=0.802$).

Cerebrospinal fluid could not be obtained from the confirmed case due to the comatose state. Blood samples from the confirmed case were culture-negative, likely attributed to prior administration of antibiotics before sampling. We successfully cultured and isolated three *Nm* strains from the 24 *Nm* nucleic acid PCR(+) close contacts. Through third-generation, whole-genome sequencing, we identified a 1655 *Nm* sequence type (ST-1655) within clonal complex 23 (CC-23), closely related to strains found in eight cases of serogroup Y *Nm* previously documented in Guangdong Province.

We conducted an evaluation of vaccination status and identified that neither the confirmed case nor any of their close contacts had a history of receiving MenY-containing vaccines. Given that the school population comprised peers or older individuals compared to the confirmed case, and MenY-containing vaccines were initially approved for use in China in 2008 and are not part of the routine immunization program, we deduced that MenY-containing vaccine coverage among the school population was likely negligible. Through the utilization of the immunization information system, we determined that MenY-containing vaccine coverage was meager in Zengcheng District, with only 3.01% of children aged 2–6 years and 0.45% of children aged 7–18 years having received a MenY-containing vaccine.

Results of antimicrobial susceptibility testing on *Nm* strains and comprehensive control measures taken in the investigation were shown in the Supplementary Material (available at https://weekly.chinacdc.cn/).

DISCUSSION

Invasive meningococcal disease (IMD) is characterized by its rapid onset and poor prognosis, with untreated cases having a case fatality rate of up to 80% and 4%–20% when appropriately treated (*1*). *Nm* comprises twelve serogroups, with serogroups A, B, C, W, X, and Y accounting for almost all IMD cases. Global IMD incidence has generally decreased due to effective meningococcal immunization programs and temporal trends (*2*). In China, the occurrence of meningococcal meningitis has reached historically low

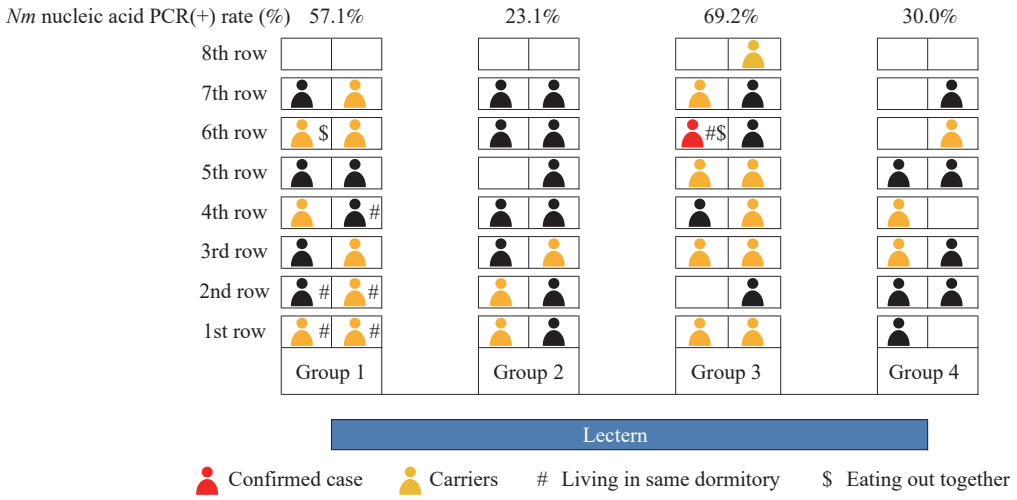

FIGURE 2. Seating patterns in the confirmed case's classroom showing *Nm* nucleic acid PCR(+) status of classmates.
Abbreviation: PCR=polymerase chain reaction; *Nm=Neisseria meningitidis*.

levels (*3*–*4*). Notably, there has been ongoing diversification of global meningococcal serogroups. Surveillance data from China over the last decade reveal a shift in the predominant epidemic serogroup of *Nm* from A to C and B, along with an increase in cases of serogroups Y and W (*3*).

The confirmed case in this outbreak exhibited an acute onset of illness that quickly escalated to a severe state, a characteristic presentation of fulminant meningococcal meningitis. The rapid advancement to irreversible physical damage underscores the potent pathogenicity of serogroup Y *Nm*. Despite the current low incidence of meningococcal meningitis, the gravity of the illness, poor outcomes, and potential sequela warrant significant attention, even in sporadic cases. Timely detection and treatment are crucial once *Nm* infection is suspected.

The outbreak analysis revealed that serogroup Y *Nm*, similar to other *Nm* serogroups, commonly exists in a carrier state. *Nm* colonizes the human respiratory tract as an opportunistic pathogen, which can be challenging to detect but can be present in respiratory secretions. Carriers play a crucial role as potential sources of infection. Therefore, it is imperative that upon diagnosing an *Nm* infection, efforts be made to identify other infected individuals and implement prophylactic measures to curtail further transmission.

Nm is a fragile pathogen with limited viability outside the host, requiring specific time and space conditions for survival and transmission. Our investigation demonstrates that individuals carrying *Nm* are frequently identified among classmates or roommates of confirmed case, highlighting the role of sustained close contact in shared environments as a significant transmission risk factor. An analysis of seating arrangements within the confirmed case's classroom revealed that both the classroom groups of the confirmed case and his roommates exhibited higher rates of *Nm* carriage compared to other classroom groups. This increased risk of infection could be attributed to cohabitation with a confirmed case, as evidenced by the presence of three PCR(+) roommates serving as potential sources of infection. Furthermore, the confirmed case's frequent visits to his roommates' classroom group may have contributed to this observed similarity in infection risk. The findings underscore the importance of close contact in fostering *Nm* transmission. Therefore, during a meningococcal meningitis outbreak, individuals with prolonged exposure to a case in shared spaces should be prioritized for active surveillance, monitoring, and appropriate medical intervention.

The confirmed case in this outbreak marked the ninth reported instance of serogroup Y meningococcal meningitis in Guangdong Province since the initial serogroup Y case was documented in Dongguan City in 2019 (*5*). The genotype observed in this outbreak aligns with what has been documented in Hunan and other provincial-level administrative divisions (PLADs) of China (*5*–*6*). Pathogen surveillance data indicates that there were no reports of serogroup Y meningococcal meningitis in China before 2014 (*4*). However, since then, five cases of serogroup Y meningitis in Guangdong Province since the initial serogroup Y case was documented in Dongguan City in 2019 (*5*). The genotype observed in this outbreak aligns with what has been documented in Hunan and other provincial-level administrative divisions (PLADs) of China (*5*–*6*). Pathogen surveillance data indicates

that there were no reports of serogroup Ymeningococcal meningitis have been reported in Tianjin Municipality, Guangdong Province, Zhejiang Province, and Ningxia Hui Autonomous Region from 2015 to 2019 (*3*,*5*,*7*), highlighting a delayed emergence of serogroup Y meningococcal meningitis in China. In contrast, serogroup Y was already prevalent worldwide by 2011 and has been reported in 23 countries, emerging as a predominant epidemic serotype in North and South America and Northern Europe (*8*–*9*).

Presently, the principal clonal complexes (CCs) of the six major highly pathogenic serogroups causing global epidemics are A (CC-5, CC-7), B (CC-41/44, CC-32, CC-18, CC-269, CC-8, CC-35), C (CC-11), Y (CC-23, CC-167), W-135 (CC-11), and X (CC-181) (*10*). In China, all serogroup Y cases reported belong to CC-23, consistent with the epidemic clonal complex of serogroup Y (CC-23, CC-167). With an increasing number of reported cases and affected regions of serogroup *Nm*, ongoing etiological surveillance and population carrier monitoring are imperative for effective prevention and control of meningococcal meningitis.

Immunization rates with Men-A-C-containing vaccines (MPV-A and MPV-AC) are notably high due to their inclusion in the NIP. Conversely, MenY-containing vaccines (MPV-ACYW135 and MPCV-ACYW135) are not part of the routine immunization schedule and were only granted approval in China in 2008 and 2021, respectively. Seroprevalence studies conducted across various Chinese regions have shown relatively low levels of immunity against serogroup Y *Nm*, ranging from 10% to 60%. An unpublished investigation conducted in Guangdong revealed a 35% *Nm* IgG seroprevalence rate, suggesting suboptimal population immunity.

Based on the findings of this investigation, we propose the reinforcement of etiological surveillance and population carrier surveillance for *Nm*. Notably, *Nm* serogroups in China are undergoing continuous change and diversification. However, the current NIP vaccines only target serogroups A and C, omitting serogroups B, Y, and W. Therefore, the research and development of multivalent meningococcal vaccines and the refinement of immunization strategies are crucial for effective prevention and control of *Nm* infections in China.

Conflicts of interest: No conflicts of interest.

Acknowledgements: Dr. Lance Rodewald for refining the language of this manuscript.

Funding: Chinese Field Epidemiology Training Program.

doi: 10.46234/ccdcw2024.048

Corresponding author: Lei Luo, llyeyq@163.com.

[1] Chinese Field Epidemiology Training Program, Chinese Center for Disease Control and Prevention, Beijing, China; [2] Zhuhai Center for Disease Control and Prevention, Zhuhai City, Guangdong Province, China; [3] Guangdong Center for Disease Control and Prevention, Guangzhou City, Guangdong Province, China; [4] Guangzhou Center for Disease Control and Prevention, Guangzhou City, Guangdong Province, China; [5] Institute of Public Health, Guangzhou Medical University & Guangzhou Center for Disease Control and Prevention, Guangzhou City, Guangdong Province, China; [6] Department of the National Immunization Programme, Chinese Center for Disease Control and Prevention, Beijing, China.
[&] Joint first authors.

Submitted: November 02, 2023; Accepted: March 18, 2024

REFERENCES

1. Wang B, Santoreneos R, Giles L, Afzali HHA, Marshall H. Case fatality rates of invasive meningococcal disease by serogroup and age: A systematic review and meta-analysis. Vaccine 2019;37(21):2768 – 82. https://doi.org/10.1016/j.vaccine.2019.04.020.
2. Parikh SR, Campbell H, Bettinger JA, Harrison LH, Marshall HS, Martinon-Torres F, et al. The everchanging epidemiology of meningococcal disease worldwide and the potential for prevention through vaccination. J Infect 2020;81(4):483 – 98. https://doi.org/10.1016/j.jinf.2020.05.079.
3. Li JH, Wu D, Wen N, Zheng H, Shi W, Xu L, et al. Serogroup distribution of meningococcal meningitis in China, 2015–2019. Chin J Vaccines Immun 2020;26(3):241-4. https://d.wanfangdata.com.cn/periodical/zgjhmy202003001. (In Chinese).
4. Li JH, Li YX, Wu D, Ning GJ, Shao ZJ, Yin ZD. Epidemiological characteristics of meningococcal meningitis and switching trend of serogroups of Neisseria meningitidis in China, 2006–2014. Chin J Vaccines Immun 2015;21(5):481-5. https://d.wanfangdata.com.cn/periodical/zgjhmy201505001. (In Chinese).
5. Zhang LP, Ye XY, Xiong HZ, Huang Y, Ye XF, Zhang QL. Analysis on the first infection case of Neisseria meningitidis Y clonal complex 23 in China. Dis Surveill 2020;35(7):664 – 7. https://doi.org/10.3784/j.issn.1003-9961.2020.07.023.
6. Xia X, Fang ML, Qin D, He ZX, Gao LD, Zhan ZF. Etiological characteristics of strains from cases of epidemic cerebrospinal meningitis due to newly isolated *Neisseria meningitidis* serogroups X and Y in Hunan Province. Pract Prev Med 2021;28(11):1295 – 8. https://doi.org/10.3969/j.issn.1006-3110.2021.11.004.
7. Guo LC, Liu XC, Xu QY, Liu YS, Cai Y, Jiang GY, et al. Epidemiological analysis on serogroup Y *Neisseria meningitidis* firstly isolated from patient in Tianjin. Chin J Prev Med 2016;50(9):825 – 7. https://doi.org/10.3760/cma.j.issn.0253-9624.2016.09.015.
8. Bröker M, Jacobsson S, Kuusi M, Pace D, Simões MJ, Skoczynska A, et al. Meningococcal serogroup Y emergence in Europe: update 2011. Hum Vaccines Immunother 2012;8(12):1907 – 11. https://doi.org/10.4161/hv.21794.
9. Sharip A, Sorvillo F, Redelings MD, Mascola L, Wise M, Nguyen DM. Population-based analysis of meningococcal disease mortality in the United States: 1990-2002. Pediatr Infect Dis J 2006;25(3):191 – 4. https://doi.org/10.1097/01.inf.0000202065.03366.0c.
10. Chang QZ, Tzeng YL, Stephens DS. Meningococcal disease: changes in epidemiology and prevention. Clin Epidemiol 2012;4:237 – 45. https://doi.org/10.2147/CLEP.S28410.

SUPPLEMENTARY MATERIAL

Antimicrobial Susceptible Testing

Antimicrobial susceptible testing was performed on three strains cultured and isolated from the 24 *Nm* nucleic acid PCR(+) close contacts against twelve antibiotics: Penicillin, Ampicillin, Cefotaxime, Ceftriaxone, Meropenem, Azithromycin, Minomycin, Ciprofloxacin, Levofloxacin, Trimethoprim/sulfamethoxazole (SXT25), Chloramphenicol, and Rifampicin. One strain exhibited resistance to SXT25 and was intermediate to penicillin, while the other two strains showed susceptibility to all twelve antibiotics tested. The results of antimicrobial susceptible testing on each Nm strain for 12 antibiotics were shown in Supplementary Table S1.

Comprehensive Prevention and Control Measures

Throughout the investigation, various preventive and control measures were implemented. These mainly included the active treatment of the confirmed case, administering antibiotic prophylaxis to 82 close contacts accompanied by a ten-day medical observation period, and conducting emergency vaccination of teachers and students at the school. In addition, the disinfection of epidemic spot, the training on prevention and treatment of meningococcal meningitis in medical institutions in the city, the strengthening of recent surveillance of meningococcal meningitis and the guidance on prevention and control of nosocomial infection in visiting hospitals were carried out.

During the observation period for close contacts, no instances of fever, headache, or symptoms related to meningococcal meningitis were reported. Among the close contacts, 75 individuals (91.5%) received prophylaxis (azithromycin, 0.25 g/tablet, 2 tablets once daily for 3 days). Additionally, throat swabs were collected from 10 close contacts who had previously tested PCR-positive for *Nm*, after completing 3 days of medication; all results came back negative, indicating the effectiveness of the preventive treatment. Emergency vaccination was administered using the meningococcal polysaccharide vaccine ACYW135 (MPV-ACYW135). A total of 1,244 individuals opted to receive the vaccine voluntarily, resulting in an overall coverage rate of 61.5%, with close contacts achieving a coverage rate of 75.8%.

SUPPLEMENTARY TABLE S1. Results of antimicrobial susceptible testing on Nm strains isolated and cultured.

Trial antibiotics	Strain No.		
	N23-13	N23-14	N23-15
Penicillin P	intermediate	susceptible	susceptible
Ampicillin AMP	intermediate	susceptible	susceptible
Cefotaxime CTX30	susceptible	susceptible	susceptible
Ceftriaxone CRO30	susceptible	susceptible	susceptible
Meropenem MRP	susceptible	susceptible	susceptible
Azithromycin AZM15	susceptible	susceptible	susceptible
Minomycin MN30	susceptible	susceptible	susceptible
Ciprofloxacin CIP5	susceptible	susceptible	susceptible
Levofloxacin LEV	susceptible	susceptible	susceptible
Trimethoprim/sulfameth-oxazole SXT25	resistant	susceptible	susceptible
Chloramphenicol C30	susceptible	susceptible	susceptible
Rifampicin RD5	susceptible	susceptible	susceptible

Note: All antibiotics were determined by the E-test method.

Notifiable Infectious Diseases Reports

Reported Cases and Deaths of National Notifiable Infectious Diseases — China, January 2024*

Diseases	Cases	Deaths
Plague	0	0
Cholera	0	0
SARS-CoV	0	0
Acquired immune deficiency syndrome†	3,194	1,730
Hepatitis	159,136	53
Hepatitis A	1,002	0
Hepatitis B	135,873	26
Hepatitis C	18,610	23
Hepatitis D	25	0
Hepatitis E	2,996	4
Other hepatitis	630	0
Poliomyelitis	0	0
Human infection with H5N1 virus	0	0
Measles	51	0
Epidemic hemorrhagic fever	511	1
Rabies	15	11
Japanese encephalitis	3	1
Dengue	27	0
Anthrax	7	0
Dysentery	1,689	0
Tuberculosis	60,660	383
Typhoid fever and paratyphoid fever	285	0
Meningococcal meningitis	17	1
Pertussis	15,275	5
Diphtheria	0	0
Neonatal tetanus	2	0
Scarlet fever	6,255	0
Brucellosis	4,207	0
Gonorrhea	9,112	1
Syphilis	56,658	6
Leptospirosis	19	0
Schistosomiasis	5	0
Malaria	254	3
Human infection with H7N9 virus	0	0
Monkey pox§	97	0
Influenza	2,988,914	3
Mumps	5,272	0

Continued

Diseases	Cases	Deaths
Rubella	45	0
Acute hemorrhagic conjunctivitis	3,039	0
Leprosy	24	0
Typhus	68	0
Kala azar	33	0
Echinococcosis	438	0
Filariasis	0	0
Infectious diarrhea[¶]	85,963	0
Hand, foot and mouth disease	26,382	0
Total	3,427,657	2,198

* According to the National Bureau of Disease Control and Prevention, not included coronavirus disease 2019 (COVID-19).
† The number of deaths of acquired immune deficiency syndrome (AIDS) is the number of all-cause deaths reported in the month by cumulative reported AIDS patients.
§ Since September 20, 2023, Monkey pox was included in the management of Class B infectious diseases.
¶ Infectious diarrhea excludes cholera, dysentery, typhoid fever and paratyphoid fever.
The number of cases and cause-specific deaths refer to data recorded in National Notifiable Disease Reporting System in China, which includes both clinically-diagnosed cases and laboratory-confirmed cases. Only reported cases of the 31 provincial-level administrative divisions in Chinese mainland are included in the table, whereas data of Hong Kong Special Administrative Region, Macau Special Administrative Region, and Taiwan, China are not included. Monthly statistics are calculated without annual verification, which were usually conducted in February of the next year for de-duplication and verification of reported cases in annual statistics. Therefore, 12-month cases could not be added together directly to calculate the cumulative cases because the individual information might be verified via National Notifiable Disease Reporting System according to information verification or field investigations by local CDCs.

doi: 10.46234/ccdcw2024.039

Youth Editorial Board

Indexed by Science Citation Index Expanded (SCIE), Social Sciences Citation Index (SSCI), PubMed Central (PMC), Scopus, Chinese Scientific and Technical Papers and Citations, and Chinese Science Citation Database (CSCD)

The inauguration of *China CDC Weekly* is in part supported by Project for Enhancing International Impact of China STM Journals Category D (PIIJ2-D-04-(2018)) of China Association for Science and Technology (CAST).

CCDC weekly

Vol. 6 No. 12 Mar. 22, 2024

Responsible Authority
National Disease Control and Prevention Administration

Sponsor
Chinese Center for Disease Control and Prevention

Editing and Publishing
China CDC Weekly Editorial Office
No.155 Changbai Road, Changping District, Beijing, China
Tel: 86-10-63150501, 63150701
Email: weekly@chinacdc.cn

CSSN
ISSN 2096-7071
CN 10-1629/R1